Copyright Warning & Restrictions

The copyright law of the United States (Title 17, United States Code) governs the making of photocopies or other reproductions of copyrighted material.

Under certain conditions specified in the law, libraries and archives are authorized to furnish a photocopy or other reproduction. One of these specified conditions is that the photocopy or reproduction is not to be "used for any purpose other than private study, scholarship, or research." If a, user makes a request for, or later uses, a photocopy or reproduction for purposes in excess of "fair use" that user may be liable for copyright infringement,

This institution reserves the right to refuse to accept a copying order if, in its judgment, fulfillment of the order would involve violation of copyright law.

Please Note: The author retains the copyright while the New Jersey Institute of Technology reserves the right to distribute this thesis or dissertation

Printing note: If you do not wish to print this page, then select "Pages from: first page # to: last page #" on the print dialog screen

ABSTRACT

SPARSE METHODS FOR BLIND SOURCE SEPARATION OF FREQUENCY HOPPING RF SOURCES

by
Anushreya Ghosh

Blind source separation (BSS) is performed on frequency hopping (FH) sources. These radio frequency (RF) signals are observed by a uniform linear array (ULA) over a Spatial Channel Model (SCM) in four different propagation environments: (*i*) line-of-sight (LOS), (*ii*) single-cluster, (*iii*) multiple-cluster, and (*iv*) LOS with interference. The sources are spatially sparse, and their activity is intermittent and assumed to follow a hidden Markov model (HMM). BSS is achieved by utilizing direction of arrival (DOA) of the sources and clusters. A sparse detection framework is applied to obtain estimates of the sources' FH and DOA patterns. The solutions are binned according to a frequency grid and a DOA dictionary. A method is proposed to reduce the effect of falsely detected active sources and mitigate the effects of interference, by leveraging the activity model of the intermittent sources. The proposed method is a state filtering technique, referred to as hidden state filtering (HSF), and is used to improve BSS performance. Multiple activity patterns associated with different DOAs are considered "similar" if they match over a prescribed fraction of the time samples. A method pairing DOA and FH estimates associates the FH patterns to specific sources via their estimated DOAs. Numerical results demonstrate that the proposed algorithm is capable of separating multiple spatially sparse FH sources with intermittent activity, by providing estimates of their FH patterns and DOA.

SPARSE METHODS FOR BLIND SOURCE SEPARATION OF FREQUENCY HOPPING RF SOURCES

by
Anushreya Ghosh

A Dissertation
Submitted to the Faculty of
New Jersey Institute of Technology
in Partial Fulfillment of the Requirements for the Degree of
Doctor of Philosophy in Electrical Engineering

Helen and John C. Hartmann Department of
Electrical and Computer Engineering

May 2023

APPROVAL PAGE

SPARSE METHODS FOR BLIND SOURCE SEPARATION OF FREQUENCY HOPPING RF SOURCES

Anushreya Ghosh

Dr. Alexander M. Haimovich, Dissertation Advisor — Date
Distinguished Professor, Department of Electrical and Computer Engineering, NJIT

Dr. Ali Abdi, Committee Member — Date
Professor, Department of Electrical and Computer Engineering, NJIT

Dr. Joerg Kliewer, Committee Member — Date
Professor, Department of Electrical and Computer Engineering, NJIT

Dr. Alex Dytso, Committee Member — Date
Staff Engineer, Qualcomm Inc.

Dr. Osvaldo Simeone, Committee Member — Date
Professor, Department of Engineering, King's College, London

BIOGRAPHICAL SKETCH

Author: Anushreya Ghosh

Degree: Doctor of Philosophy

Date: May 2023

Undergraduate and Graduate Education:

- Doctor of Philosophy in Electrical Engineering,
  New Jersey Institute of Technology, Newark, NJ, 2023
- Master of Science in Electrical Engineering,
  New Jersey Institute of Technology, Newark, NJ, 2019
- Bachelor of Science in Electronics and Communication Engineering,
  West Bengal University of Technology, India, 2017

Major: Electrical Engineering

Presentations and Publications:

A. Ghosh, A. Dong, A. Haimovich, O. Simeone and J. Dabin, "Blind Source Separation of Intermittent Frequency Hopping Sources over LOS and NLOS channels", *IEEE Transactions on Wireless Communications*, Submitted, 2023.

A. Ghosh, A. Haimovich, and J. Dabin, "Interference Mitigation in Blind Source Separation by Hidden State Filtering", *57th Annual Conference on Information Sciences and Systems (CISS)*, Baltimore, MA, USA, pp. 1-6, 2023.

A. Dong, **A. Ghosh**, A. Haimovich and J. Dabin, "Sparse Recovery of Intermittent Frequency Hopping Signals Aided by DOA", *54th Annual Conference on Information Sciences and Systems (CISS)*, Princeton, NJ, USA, pp. 1-6, 2020.

A. Ghosh, "Blind source separation using dictionary learning over time-varying channels", *MS Thesis*, Electrical and Computer Engineering, New Jersey Institute of Technology, USA, 2019.

Hope and curiosity about the future seemed better than guarantees. The unknown was always so attractive to me...and still is.

Hedy Lamarr,
Innovator of concepts behind Frequency Hopping,
Bluetooth, GPS and Wi-Fi. Also, a famous actress.

ACKNOWLEDGMENT

This work is made possible because of the guidance of Dr. Alexander M. Haimovich whose support throughout the research culminated in the fulfillment of this dissertation. I have learned a lot from him, both in my approach towards engineering research; and in how to be a better academic and professional. The talks we had throughout the years will always hold a special place in my heart.

Special thanks are also due to my PhD Committee members, Drs. Ali Abdi, Alex Dytso, Osvaldo Simeone and Joerg Kliewer for their advice and support as well.

I gratefully acknowledge the funding sources that made my research possible. My work was supported in part by the U.S. Department of Defense (Navy - Naval Information Warfare Center) under Agreements no. N66001-20-P-6010 and N66001-21-P-6576. I also appreciate the funding from the Department of Electrical and Computer Engineering.

Throughout the time that I have been a part of the Department of Electrical and Computer Engineering, Ms. Monteria Bass and Ms. Kathleen Bosco have been integral parts of my life. They were always ready to help, be it a professional or personal issue. To anyone needing help, I pray you find people as patient as them.

Thanks are due to my colleagues at the Center for Wireless Information Processing. Dr. Annan Dong for his help during the very first days of my research career, and for always answering when I reached out to him. Dr. Wei Jiang is one of my closest friend and ally. Drs. Malihe Aliasgari and Sarah Obead helped me piggy-back their dissertation experience, and in the process made my life easier. Ian Zieder and Kyle Wensell helped me acclimate to the Center and were there whenever I needed a friendly ear.

I have lots of love and gratefulness for Arunima Pal, who has seen me grow in to the person I am now, and contributed heavily to it. Mirana Alam was the first

friend I made at NJIT. She has been there for me through some of the most difficult times of my life, and I am eternally grateful to her. I am also thankful for the help Esthi Zipori has given me through the years.

Special thanks go out to Alexander Greyson who kept me sane through numerous instances of self doubt and bouts of worry. You deserve a trophy for the calm you bring in my life.

My mother, Uma Mitra Ghosh, was the first real-life STEM heroine I have known in my life. Thanks to her, and my sister Dr. Anasooya Ghosh, for the support and the push I needed to pursue a career in STEM. And thanks to my nephew Pi, who heard a diluted summary of what I do and said, "Cool."

TABLE OF CONTENTS

Chapter **Page**

1 INTRODUCTION 1

1.1 Related Work 3

1.2 Main Contributions 6

2 SYSTEM MODEL 8

2.1 Source Model 9

2.2 Observation Model 11

2.2.1 Line-of-Sight (LOS) propagation environment 14

2.2.2 Single-cluster propagation environment 15

2.2.3 Multiple-cluster propagation environment 17

2.2.4 LOS propagation environment with interference 19

3 SOURCE PARAMETER AND PATTERN ESTIMATION 21

3.1 FH Estimation 23

3.2 DOA estimation 25

3.3 Hidden State Filtering (HSF) 26

3.3.1 Forward-Backward procedure 27

3.3.2 Individually most probable states 29

3.3.3 Most probable sequence of states 30

3.3.4 Learning HMM parameters 33

3.4 Pairing 36

4 NUMERICAL RESULTS 38

5 CONCLUSION 53

Appendix A VITERBI ALGORITHM 56

REFERENCES 58

LIST OF FIGURES

Figure		Page
2.1	Uniform linear array with J sensors.	8
2.2	Intermittent source activity.	9
2.3	Hidden Markov model for a source.	10
2.4	Source activity of two FH sources.	11
2.5	LOS propagation environment for one source.	14
2.6	Single-cluster propagation environment for one source.	15
2.7	Multiple-cluster propagation environment for one source.	17
2.8	Intermittent source activity along with interference.	19
3.1	Block diagram of the proposed algorithm to separate multiple FH sources and assign source labels.	22
4.1	FH truth and estimation for two sources. ($M = 10$ sensors).	39
4.2	True DOA activity and estimation for two LOS sources with intermittent source activity. ($M = 10$ sensors).	39
4.3	P_d versus P_{fa} of FH estimates (5 sources, $J = 20$ sensors, $T = 1000$ samples, SNR = 10 dB).	41
4.4	P_d versus P_{fa} of activity with and without HSF for LOS propagation environment (5 sources, $J = 20$ sensors, $T = 1000$ samples, SNR = 10 dB).	42
4.5	P_d versus P_{fa} of activity in presence of stronger sources for LOS propagation environment (5 sources, $J = 20$ sensors, $T = 1000$ samples).	43
4.6	P_d versus P_{fa} of activity with and without HSF for single-cluster propagation environment (5 sources, $J = 20$ sensors, $T = 1000$ samples, SNR = 10 dB).	44
4.7	P_d versus P_{fa} of activity with and without HSF for 2-cluster propagation environment (5 sources, $J = 20$ sensors, $T = 1000$ samples, SNR = 10 dB, $\varrho = 1$).	45
4.8	P_d versus P_{fa} of activity with and without HSF for 2-cluster propagation environment (5 sources, $J = 20$ sensors, $T = 1000$ samples, SNR = 10 dB, $\varrho = 0.9$).	46

LIST OF FIGURES
(Continued)

Figure **Page**

4.9 P_d versus P_{fa} of activity with and without HSF for 2-cluster propagation environment (5 sources, $J = 20$ sensors, $T = 1000$ samples, SNR = 10 dB, $\varrho = 0.95$). 46

4.10 P_d versus P_{fa} of paired activity with and without HSF (5 sources, $J = 20$ sensors, $T = 1000$ samples, SNR = 10 dB, $\varrho = 0.95$). 47

4.11 P_d when $P_{fa} = 0.15$ versus number of intermittent sources detected active during observation interval in the LOS propagation environment ($J =$ 20 sensors, $T = 1000$ samples, SNR = 10 dB). 48

4.12 P_d versus P_{fa} for activity for LOS propagation environment with interference with and without HSF (5 intermittent sources with SNR = 10 dB, 1 jammer with SNR = 20 dB, $J = 20$ sensors, $T = 1000$ samples). 49

4.13 P_{fa} of activity when $P_{fa} = 0.6$ versus Jammer to Signal Ratio in dB (5 intermittent sources with SNR = 10 dB, 1 jammer, $J = 20$ sensors, T = 1000 samples). 50

4.14 P_d versus P_{fa} for activity (5 intermittent sources with SNR = 10 dB, 1 jammer with SNR = 20 dB, $J = 20$ sensors, $T = 1000$ samples). . . . 51

4.15 P_d when $P_{fa} = 0.6$ versus number of intermittent sources detected active in LOS propagation environment with interference ($J = 20$ sensors, T = 1000 samples, SNR of jammer = 20 dB, SNR of sources = 10 dB). . 52

CHAPTER 1

INTRODUCTION

Frequency hopping (FH) spread spectrum signals have been widely studied and adopted for wireless communications thanks to a multitude of advantages, such as their low probability of detection and their inherent robustness to jamming [1–3]. Estimating and tracking parameters of multiple FH signals have important applications in both civilian and military fields, such as collision avoidance [4, 5], cognitive radio [6, 7], and interception of non-cooperative communications [8, 9]. The estimation of FH signal parameters for the purpose of intercepting non-cooperative sources is the focus of this work.

The FH sources assumed in this work transmit at frequencies that change pseudo-randomly within a block of spectrum. Parameters such as hop time, hopping pattern, and frequencies are random and unknown at the receiver. The localization and separation of multiple FH sources without knowledge of these parameters is posed as a blind source separation (BSS) problem [10].

To perform BSS of multiple FH sources, it is not sufficient to produce a frequency versus time map of the power of the observed signals, but also to associate the signals to physical sources. We refer to the task of associating frequency hops to a source as the problem of labeling of FH signals. Since frequency hop estimates cannot determine which of several sources transmitted the signal, it is necessary to estimate information that is source specific and extraneous to the FH pattern. To do so, one can leverage the knowledge that all signals transmitted by a source via line-of-sight (LOS) propagation have the same direction of arrival (DOA) information.

Estimating the DOAs of the sources is made more challenging if signals are received via multipath propagation. Measurement data analysis in [11] demonstrates

that nearby physical structures act as secondary sources, forming separable clusters with narrow angular spread around them [12–14]. Several cluster-based channel models can be found in the literature, such as the 3GPP Spatial Channel Model (SCM) [15–17], WINNER II [18], and the 3GPP Clustered Delay Line (CDL) model [19]. In [15–17], the SCM is defined for different scenarios, namely suburban macro, urban macro and urban micro. The urban micro channel propagation environment deals with LOS sources, and the other two propagation environments take the effects of multipath propagation into account and deal with non line-of-sight (NLOS) sources. In this work, signals are observed over channels that follow the SCM model for four propagation environments: (*i*) LOS, (*ii*) single-cluster, (*iii*) multiple-cluster, and (*iv*) LOS with interference.

1.1 Related Work

Independent Component Analysis (ICA) [21] has been used to solve the BSS problem in wireless networks [22, 23]. Reference [24] uses ICA in MIMO systems with time-varying channels by changing the data block length of received signals. The Equivariant Adaptive Separation using Independence (EASI) algorithm [25] that utilizes ICA has been used to perform source separation under the assumption that at any time instant the components of the source signals are mutually statistically independent and have unit variance. Algorithms that use EASI as a basis have been developed as well [26, 27]. However, ICA and ICA-based techniques assume equal number of sources and sensors in the system, and further assume that the sources are always active. ICA is not applicable in BSS problems where sources turn on and off intermittently. Additionally, it is not possible to know the number of sources, and number of sensors cannot be guaranteed to be equal to the number of sources.

Among other approaches used to solve the BSS problem of FH sources is time-frequency analysis (TFA) [33–36]. TFA methods are applied to study representations of the received FH signal in both time and frequency domains. However, as captured by the uncertainty principle, it is not possible to reach good time and frequency resolutions simultaneously [37]. TFA methods also suffer from cross-term interference and spectral leakage, resulting in high SNR requirements [38].

TFA-based methods have been used as exploratory tools towards more refined solutions to blind estimation of hop timings and frequencies. When only one FH signal is present, authors in [39] proposes to first apply TFA to estimate the hopping pattern, and, subsequently, a particle filter operates on the initial estimation. The initial estimation of hopping patterns in [39] depends on TFA-based methods, and therefore has high signal-to-noise (SNR) requirements. A blind maximum-likelihood (ML)-based iterative algorithm is proposed in [40] that estimates hop timing and frequency hops for a single-user. The ML-based algorithm has been shown to have lower SNR

requirements than TFA-based approaches in [40]. However, the formulation in [40] cannot be generalized to multiple FH signals.

For multiple FH signals, the method proposed in [41] implements a dynamic programming-based ML estimator that yields estimates of joint hop timings and frequencies. An approach based on sparse linear regression is introduced to estimate the hop timings and frequencies of multiple FH signals in [21]. Each hop in [41, 42] is treated as a distinct source. This method is not suitable for grouping frequency hops according to physical sources. To associate frequency hops to a source and label FH signals, the DOAs of the sources are estimated as they are source specific extraneous to the FH pattern.

A two-step approach is introduced to estimate DOA, hop timings, and frequency hops for multiple sources in [43]. A TFA method is applied to signals received by a uniform linear array (ULA) to identify a hop-free duration for DOA estimation. After the DOAs are recovered, joint estimation of hop timings and frequencies is performed for each signal originating from the same DOA. However, as mentioned earlier, approaches such as [43] that rely on TFA-based approaches for initial estimations suffer from cross-terms interference and high SNR requirements. The joint estimation of FH parameters and DOA for multiple sources is studied in [44–47] under the assumption that all sources are active throughout the entire observation interval. Additionally, the hop periods are assumed uniform [47]. None of the approaches in [44–47] are able to incorporate sources that are sparse spatially and have intermittent activity, and probabilistic source models, such as Markov models.

BSS of spatially sparse sources that have intermittent activity has been studied in [28] where the sources transmit over slow flat-fading channels, and in [29] where the channel is flat-fading and time-varying. BSS of intermittent sources has also been studied in [30] - [31] where the sources are frequency hopping, and transmit over LOS channels. In [30], signals transmitting over LOS channels are received by an ULA

of sensors, and their DOAs are used as the criterion of source separation; and [31] studies three different channel propagation environments with LOS, single-cluster and multiple-cluster propagation environments. Reference [32] considers how BSS of intermittent sources will be affected in the presence of interference.

1.2 Main Contributions

In this work, a BSS problem is solved in which source separation over LOS and NLOS channels relies on determining FH and source activity jointly for sources that are spatially sparse and have intermittent activity. Sources are spatially sparse in the sense that only a fraction of the sources is active at a given time instant, and is intermittent in the sense that the cumulative time over which a source is active is only a fraction of the total period of observation [48]. Activity is also "smooth", i.e., on-off patterns of sources vary slowly.

An approach is proposed which consists of a FH estimation stage, a DOA estimation stage, hidden state filtering (HSF) to refine DOA estimates, and a pairing stage that combines information from the previous stages to associated FH patterns with physical source. The FH and DOA estimation problems are formulated as optimizations in a sparse representation framework. For the FH and DOA estimation stages, dictionaries are formulated as grids of FH frequencies and DOAs, respectively. Refined DOA estimates are obtained by applying HSF. HSF is performed by inferring a hidden Markov model (HMM) state sequence from observed data. Two different types of HSF are implemented in this work: (i) Most Probable Estimate (MPE) and (ii) maximum a posteriori (MAP) estimate. The pairing stage extracts components of the FH and DOA dictionaries that were found to be active in the FH and DOA estimation stages, and creates a new dictionary of paired FH and DOA values. Using the new dictionary, a sparse representation problem is formulated to pair the FH and DOA estimates.

Four propagation environments are observed in this work. First, the FH sources are assumed to be LOS sources. Second, the sources appear as single clusters. Thirdly, the FH sources are observed under multipath conditions, where they appear as multiple clusters. And lastly, an interfering jammer is assumed active during the entire duration of observation of the sources. While the LOS sources of interest are

spatially sparse and have intermittent activity. The jammer transmits from a fixed but unknown DOA. Our goal is to use observations made by the ULA to separate the sources of interest. The HMM, used to model the spatially sparse and intermittent activity of the sources, is leveraged to enforce solutions that are "smooth", to filter out false alarms, effects of multipath, and to reduce the deleterious effect of the interference.

The main contributions of this work are as follows:

1. A sparse representation framework is introduced to obtain estimates of the frequency hops and DOA of spatially sparse RF sources with intermittent activity. Four propagation environments are observed: LOS, single-cluster, multiple-cluster and LOS with interference;
2. A method is developed to associate FH and DOA estimates of multiple sources, thus effectively achieving blind source separation;
3. Two different HSF techniques are introduced and compared;
4. Leveraging the HMM activity model of the sources, HSF is used to mitigate the effect of an interfering jammer;
5. An algorithm is developed that combines HSF with the estimation of HMM parameters, implementing the filtering without *a priori* knowledge of the HMM parameters.

The rest of the document is organized as follows. The system model with aperiodic FH and the hidden Markov source model are presented in Chapter 2. In Chapter 3, we propose the approach to separate FH, DOA and assign labels to signals transmitted from different sources. In Chapter 4, simulation based numerical results demonstrate the performance of the proposed approach and Chapter 5 reports our conclusions.

Notation: The notation $1 : T$ denotes the sequence $1, 2, \ldots, T$. Vectors are denoted by boldface lower case letters, such as $\mathbf{x}$. All vectors are assumed to be column vectors. Matrices, are denoted by boldface upper case letters, such as $\mathbf{X}$. The transpose of $\mathbf{X}$ is denoted as $\mathbf{X}'$.

CHAPTER 2

SYSTEM MODEL

Consider N sources capable of transmitting intermittent FH signals. These sources switch the carrier frequency in a randomized fashion across multiple frequency hops. Signals emitted by the sources are received at a uniform linear array (ULA) with J receiving antenna sensors spaced at uniform d-intervals, as depicted in Figure 2.1.

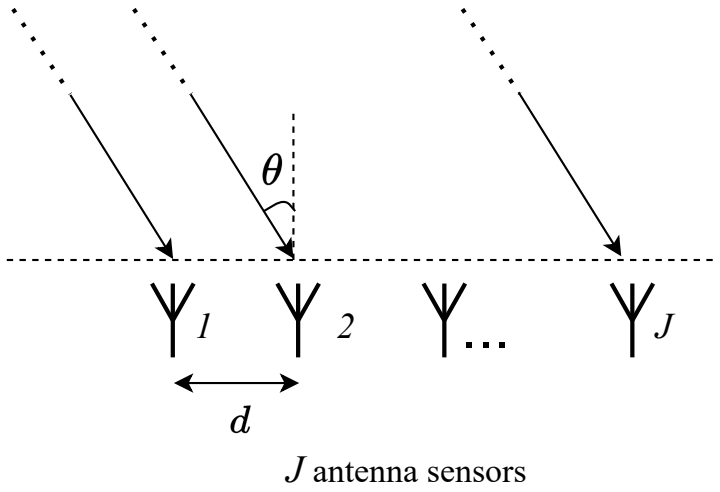

Figure 2.1 Uniform linear array with M sensors.

The total number of sources N may be larger than the number of sensors J, but, the number of active sources at any given time is lower than the number of sensors. The period of observation is T discrete time units, and, without loss of generality, the sampling interval corresponds to one time unit. The cumulative time a source is active is a small fraction of the period of observation. Sources' activity is assumed to be governed by a Markov model, as described below. On-off patterns of each source change slowly, making transitions intermittent, but smooth. The intermittent activity of the sources is discussed in Section 2.1.

2.1 Source Model

In this work, the intermittent activity of the sources is assumed to be governed by an hidden Markov model (HMM). This activity of the sources is illustrated in Figure 2.2. The activity pattern of a source is represented by a binary state sequence $s(t)$ which indicates whether at time t a source is active ($s(t) = 1$) or not ($s(t) = 0$). Since as discussed previously, a physical source may be observed over multiple DOAs, the term "DOA pattern" is used here generically, and it refers either to a physical source or an individual DOA. It is assumed that the individual DOA activity patterns associated with a physical source are "similar". Two activity patterns associated with different DOAs are considered "similar" if they match over a prescribed fraction of the time samples at which their values are 1.

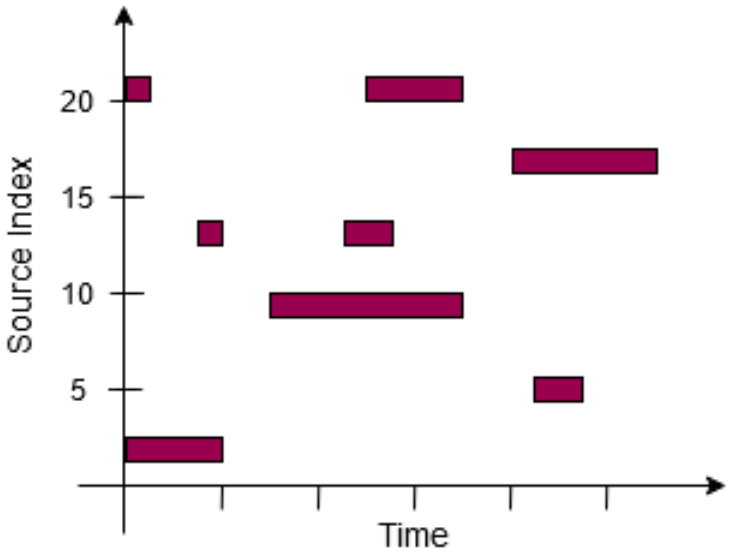

Figure 2.2 Intermittent source activity. The filled blocks denote active sources at different time instants.

A diagram representing the HMM of a source is shown in Figure 2.3. In the figure, the sequence $s(1:T)$ represents the hidden states, while the sequence $z(1:t)$ represents the observed sequence. Like state symbols, observation symbols are binary, $z(t) \in \{0, 1\}$, where $z(t) = 1$ indicates observed activity of the source at time t, and $z(t) = 0$ indicates that source was inactive at time t. In addition to states and

observations, an HMM is characterized by state transition probabilities, observation symbol probabilities, and initial state probabilities [49]. These are specified below for a source.

State transition probabilities are represented by the state transition matrix $\mathbf{A} = \{a_{ij}\}, j = 0, 1$ where the state transition probability distribution is given by $a_{ij} = P(s(t) = j | s(t-1) = i)$. Observation symbols probabilities are represented by the observation matrix $\mathbf{B} = \{b_j(k)\}, j, k = 0, 1$ where $b_j(k)$ denotes the observation symbol probability distribution in state j, $b_j(k) = P(z(t) = k | s(t) = j)$. We use the notation $b_j(z(t))$ to indicate the probability of observed value $z(t)$ conditioned on $s(t) = j$, $b_j(z(t)) = P(z(t) | s(t) = j)$. The initial state probability distribution is $\pi = \{\pi_0, \pi_1\}$, where $\pi_0 = P(s(1) = 0)$ and $\pi_1 = P(s(1) = 1)$. The parameters of an HMM are succinctly denoted by Ω, where $\Omega = (\mathbf{A}, \mathbf{B}, \pi)$.

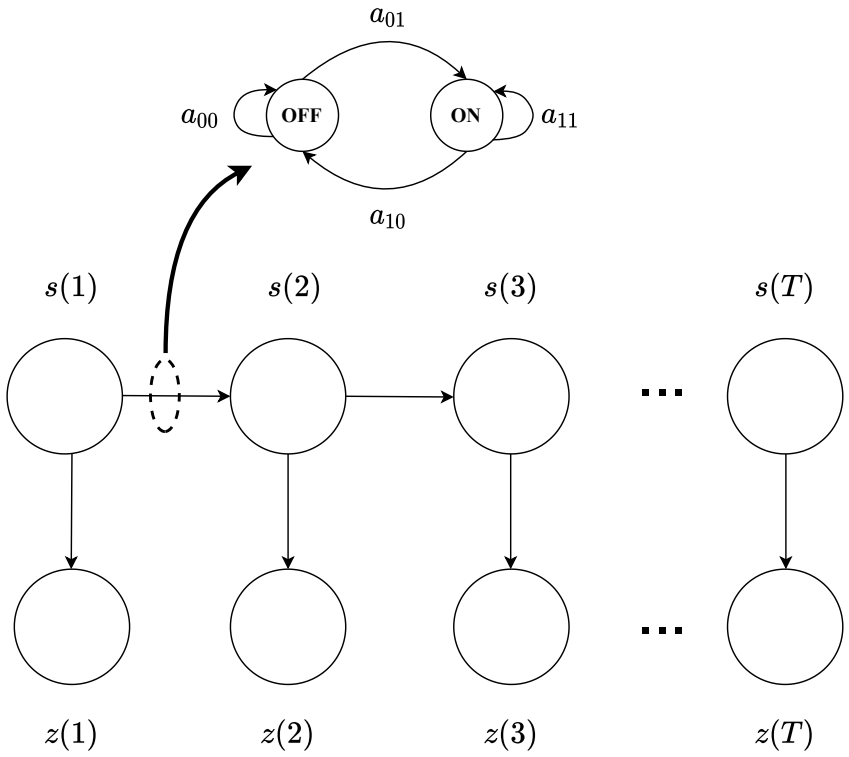

Figure 2.3 Hidden Markov Model (HMM) for a source.

2.2 Observation Model

The N intermittent sources transmit FH signals. Frequency hopping (FH) is adopted whereby sources switch the carrier frequency in a randomized fashion across multiple frequency hops. Signals emitted by the sources are received at an ULA with M receiving antenna sensors spaced at uniform d-intervals, as depicted in Figure 2.1. On-off patterns of each source change slowly, making transitions intermittent, but smooth.

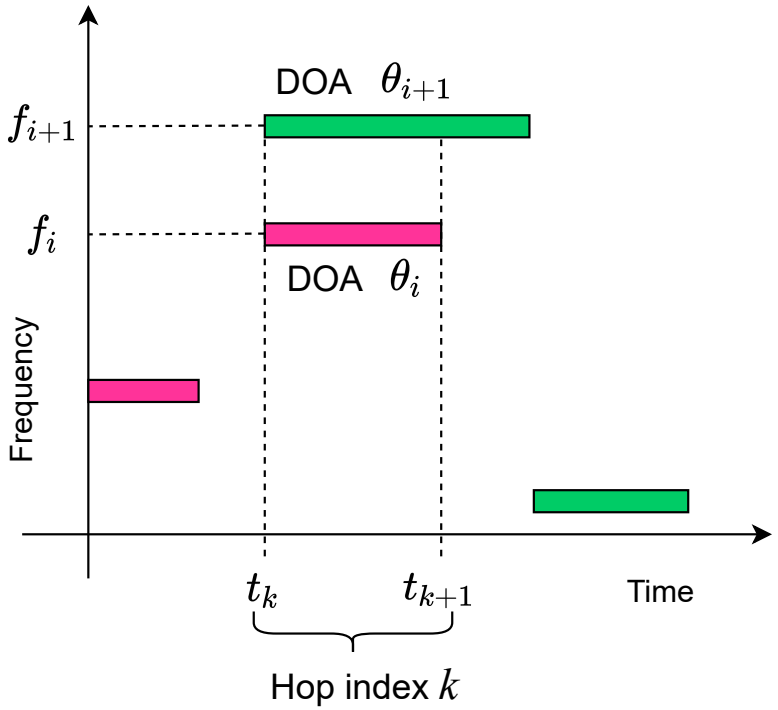

Figure 2.4 Source activity of two FH sources depicted by filled blocks with distinct shading. Time duration $t_k \leq t < t_{k+1}$ denotes a single hop with hop index k where sources with mean DOAs θ_i & θ_{i+1} transmits with frequencies f_i & f_i, respectively.

In this FH system, a hop duration is defined as the period of time between two consecutive switches of the carrier frequency of a source. The time of the k-th frequency switch is denoted t_k, and thus the duration of the corresponding hop is $(t_{k+1} - t_k)$. When multiple sources are active, the hop duration is determined by the source with the shortest time between frequency hops. An example is shown in Figure 2.4.

Assuming synchronized sensors, the signal received at the j-th sensor in the time interval $t_k \leq t < t_{k+1}$ corresponding to the k-th hop is given by

$$y(j,t) = \sum_{i=1}^{N_k} \left\{ \sum_{l=1}^{L_i} \sqrt{\frac{P_{i,l}}{M}} \sum_{m=1}^{M} c_{i,l}^{(m)}(t) a^j(\theta_{i,l}^{(m)}) \right\} h^t(f_i) + w(j,t) \tag{2.1}$$

where, N_k is the number of active sources during the k-th hop ($N_k \ll N$); L_i is the number of clusters for the i-th source; $P_{i,l}$ is the power of the l-th cluster of the i-th source which is normalized so that the total average power for all clusters is equal to one; M is the number of unresolvable multipaths per cluster that have similar characteristics. The variable $h(f_i)$ is the frequency mode of the l-th cluster of the i-th source; and $a(\theta_{i,l}^{(m)})$ is the spatial mode of the m-th multipath of the l-th cluster of the i-th source. $a^j(\cdot)$ and $h^t(\cdot)$ denote the corresponding j-th and t-th powers; $c_{i,l}^{(m)}(t)$ is the complex amplitude of the m-th multipath of the l-th cluster of the i-th source; and $w(m,t)$ is additive zero-mean complex Gaussian noise with variance σ_w^2. The frequency mode is given by $h(f_i) = e^{j2\pi f_i}$, with $f_i \in [f_{min}, f_{max}]$ being the carrier frequency of the i-th source during the k-th hop. The hop frequencies are measured relative to the carrier frequency of the receiver. The spatial mode is given by $a(\theta_{i,l}^{(m)}) = e^{j2\pi(d/\lambda)\sin(\theta_{i,l}^{(m)})}$, where d/λ is the spacing between antennae expressed in units of wavelength λ, and $\theta_{i,l}^{(m)}$ is the DOA of the m-th multipath of the l-th cluster of the i-th source. The DOA $\theta_{i,l}^{(m)}$ can be decomposed as $\theta_{i,l}^{(m)} = \theta_{i,l} + \vartheta_{i,l}^{(m)}$, where $\theta_{i,l}$ is the mean DOA of the l-th cluster of the i-th source, and $\vartheta_{i,l}^{(m)}$ is the deviation from the mean DOA, which is modeled as an i.i.d. Gaussian random variable with zero mean and variance σ_θ^2.

For hop k and corresponding time interval, $t_k \leq t < t_{k+1}$, the observations $y(j,t)$ are collected in a $J \times (t_{k+1} - t_k)$ matrix $\mathbf{Y}_k$. Combining observations across all hops, matrices $\mathbf{Y}_k$ are concatenated to form the $J \times T$ observations matrix $\mathbf{Y}$.

Four different propagation environments are observed. Equation (2.1) addresses the general formulation for all cases. The four observed propagation environments are explained in detail in the following subsections. First, the LOS propagation environment is discussed in Subsection 2.2.1. Second, the intermittent sources are observed when they appear as a single cluster with an angular spread around them. This is discussed in Subsection 2.2.2. Third, the sources are observed when they are transmit over channels with multipath components which causes the sources to appear as multiple clusters. This scenario is discussed in Subsection 2.2.3. Lastly, we observe the LOS propagation environment with interference, which is in the form of a jammer. The jammer is fixed at a particular DOA and does not undergo frequency hopping. This is discussed in Subsection 2.2.4.

2.2.1 Line-of-Sight (LOS) propagation environment

These sources are point LOS sources which arrive at the ULA with a distinct DOA for each source. The propagation environment for one LOS source ($i = 1$) is shown in Figure 2.5.

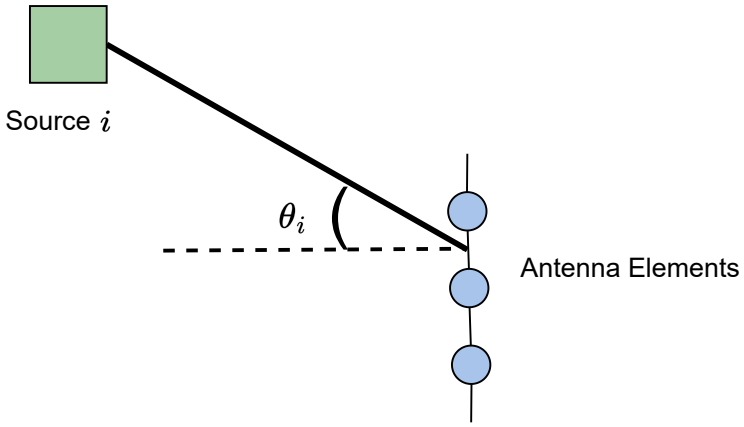

Figure 2.5 LOS propagation environment for one source.

Assuming synchronized sensors, the signal received at the j-th sensor in the time interval $t_k \leq t < t_{k+1}$ corresponding to the k-th hop is given by

$$y(j,t) = \sum_{i=1}^{N_k} \left\{ \sqrt{P_i} c_i(t) a^j(\theta_i) \right\} h^t(f_i) + w(j,t) \tag{2.2}$$

where, N_k is the number of active sources during the k-th hop ($N_k \ll N$); P_i is the power of the i-th source. The variable $h(f_i)$ is the frequency mode of the l-th cluster of the i-th source; and $a(\theta_i)$ is the spatial mode of the i-th source. $a^j(\cdot)$ and $h^t(\cdot)$ denote the corresponding j-th and t-th powers; $c_i(t)$ is the complex amplitude of the i-th source at time t; and $w(j,t)$ is additive zero-mean complex Gaussian noise with variance σ_w^2. The frequency mode is given by $h(f_i) = e^{j2\pi f_i}$, with $f_i \in [f_{min}, f_{max}]$ being the carrier frequency of the i-th source during the k-th hop. The hop frequencies are measured relative to the carrier frequency of the receiver. The spatial mode is given by $a(\theta_i) = e^{j2\pi(d/\lambda)\sin(\theta_i)}$, where d/λ is the spacing between antennae expressed in units of wavelength λ, and θ_i is the DOA of the i-th source.

2.2.2 Single-cluster propagation environment

These FH sources are not point-LOS sources, but appear as clusters with multipath components. The received signal from each source comes from the DOA which is expressed as the sum of the DOA of the cluster and a deviation based on the angular spread. The single-cluster propagation environment is depicted in Figure 2.6 for one source ($i = 1$) with one cluster ($L_i = 1$).

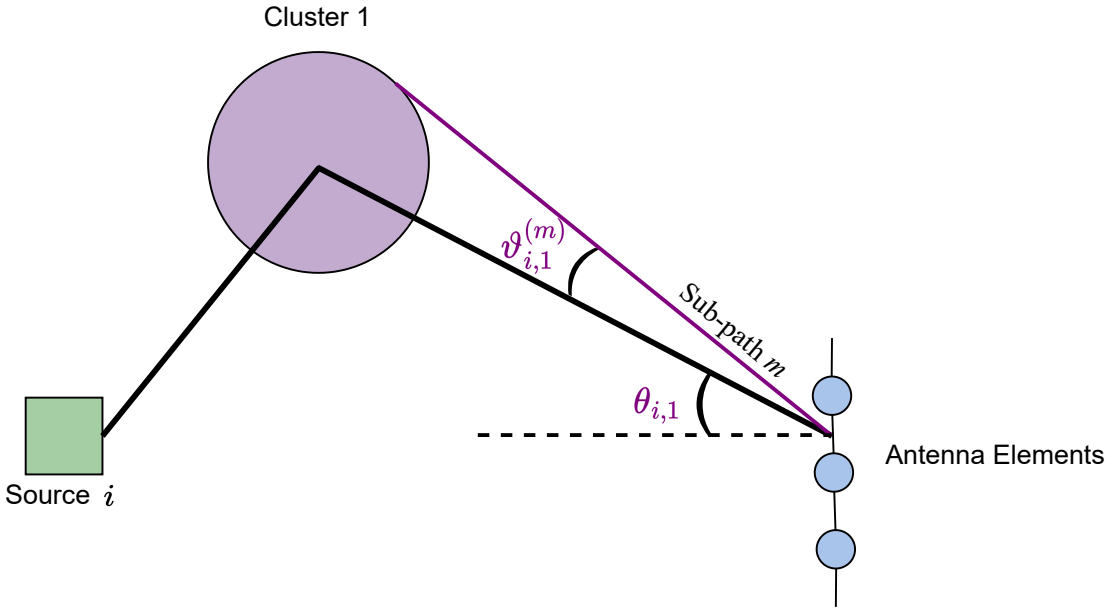

Figure 2.6 Single-cluster propagation environment for one source.

Assuming synchronized sensors, the signal received at the j-th sensor in the time interval $t_k \leq t < t_{k+1}$ corresponding to the k-th hop is given by

$$y(j,t) = \sum_{i=1}^{N_k} \left\{ \sqrt{\frac{P_{i,1}}{M}} \sum_{m=1}^{M} c_{i,1}^{(m)}(t) a^j(\theta_{i,1} + \vartheta_{i,1}^{(m)}) \right\} h^t(f_i) + w(j,t) \tag{2.3}$$

where, N_k is the number of active sources during the k-th hop ($N_k \ll N$); the number of clusters for the i-th source is one; $P_{i,1}$ is the power of the cluster of the i-th source; M is the number of unresolvable multipaths per cluster that have similar characteristics. The variable $h(f_i)$ is the frequency mode of the i-th source; and $a(\theta_{i,1}^{(m)})$ is the spatial mode of the m-th multipath of the cluster of the i-th source.

$a^j(\cdot)$ and $h^t(\cdot)$ denote the corresponding j-th and t-th powers; $c_{i,1}^{(m)}(t)$ is the complex amplitude of the m-th multipath of the one cluster of the i-th source; and $w(j,t)$ is additive zero-mean complex Gaussian noise with variance σ_w^2. The frequency mode is given by $h(f_i) = e^{j2\pi f_i}$, with $f_i \in [f_{min}, f_{max}]$ being the carrier frequency of the i-th source during the k-th hop. The hop frequencies are measured relative to the carrier frequency of the receiver. The spatial mode is given by $a(\theta_{i,1}^{(m)}) = e^{j2\pi(d/\lambda)\sin(\theta_{i,1}^{(m)})}$, where d/λ is the spacing between antennae expressed in units of wavelength λ, and $\theta_{i,1}^{(m)}$ is the DOA of the m-th multipath of the one cluster of the i-th source. The DOA $\theta_{i,1}^{(m)}$ can be decomposed as $\theta_{i,1}^{(m)} = \theta_{i,1} + \vartheta_{i,1}^{(m)}$, where $\theta_{i,1}$ is the mean DOA of the single cluster of the i-th source, and $\vartheta_{i,1}^{(m)}$ is the deviation from the mean DOA, which is modeled as an i.i.d. Gaussian random variable with zero mean and variance σ_θ^2.

2.2.3 Multiple-cluster propagation environment

Physical structures in the channel act as secondary sources, forming separable clusters [20]. The received signals from multiple-cluster source come from the DOAs of the clusters which are expressed as the sum of the mean DOA of the cluster and a deviation based on the angular spread. The multiple-cluster propagation environment is depicted in Figure 2.7 for one source ($i = 1$) with $L_i = 2$ clusters.

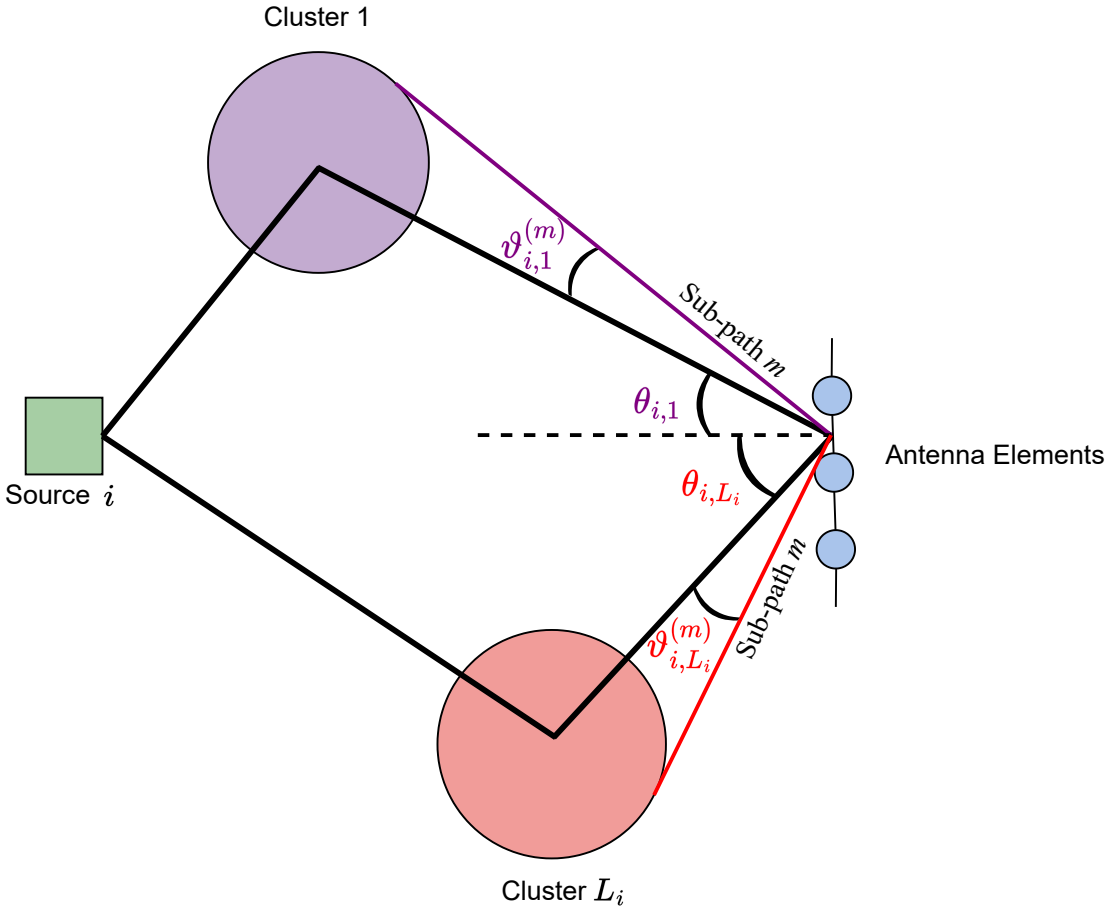

Figure 2.7 Multiple-cluster propagation environment for one source.

Assuming synchronized sensors, the signal received at the j-th sensor in the time interval $t_k \leq t < t_{k+1}$ corresponding to the k-th hop is given by

$$y(j,t) = \sum_{i=1}^{N_k} \left\{ \sum_{l=1}^{L_i} \sqrt{\frac{P_{i,l}}{M}} \sum_{m=1}^{M} c_{i,l}^{(m)}(t) a^j(\theta_{i,l}^{(m)}) \right\} h^t(f_i) + w(j,t) \tag{2.4}$$

where, N_k is the number of active sources during the k-th hop ($N_k \ll N$); L_i is the number of clusters for the i-th source; $P_{i,l}$ is the power of the l-th cluster of the i-th source which is normalized so that the total average power for all clusters is equal to one; M is the number of unresolvable multipaths per cluster that have similar characteristics. The variable $h(f_i)$ is the frequency mode of the l-th cluster of the i-th source; and $a(\theta_{i,l}^{(m)})$ is the spatial mode of the m-th multipath of the l-th cluster of the i-th source. $a^j(\cdot)$ and $h^t(\cdot)$ denote the corresponding j-th and t-th powers; $c_{i,l}^{(m)}(t)$ is the complex amplitude of the m-th multipath of the l-th cluster of the i-th source; and $w(m,t)$ is additive zero-mean complex Gaussian noise with variance σ_w^2. The frequency mode is given by $h(f_i) = e^{j2\pi f_i}$, with $f_i \in [f_{min}, f_{max}]$ being the carrier frequency of the i-th source during the k-th hop. The hop frequencies are measured relative to the carrier frequency of the receiver. The spatial mode is given by $a(\theta_{i,l}^{(m)}) = e^{j2\pi(d/\lambda)\sin(\theta_{i,l}^{(m)})}$, where d/λ is the spacing between antennae expressed in units of wavelength λ, and $\theta_{i,l}^{(m)}$ is the DOA of the m-th multipath of the l-th cluster of the i-th source. The DOA $\theta_{i,l}^{(m)}$ can be decomposed as $\theta_{i,l}^{(m)} = \theta_{i,l} + \vartheta_{i,l}^{(m)}$, where $\theta_{i,l}$ is the mean DOA of the l-th cluster of the i-th source, and $\vartheta_{i,l}^{(m)}$ is the deviation from the mean DOA, which is modeled as an i.i.d. Gaussian random variable with zero mean and variance σ_θ^2. n random variables with zero mean and variance σ_θ^2.

2.2.4 LOS propagation environment with interference

A jammer is assumed active at all time instants, in addition to the intermittent FH sources. The jammer transmits from a fixed but unknown DOA; at a constant frequency, not undergoing frequency hopping. In the presence of the jammer, the activity of the sources is illustrated in Figure 2.8.

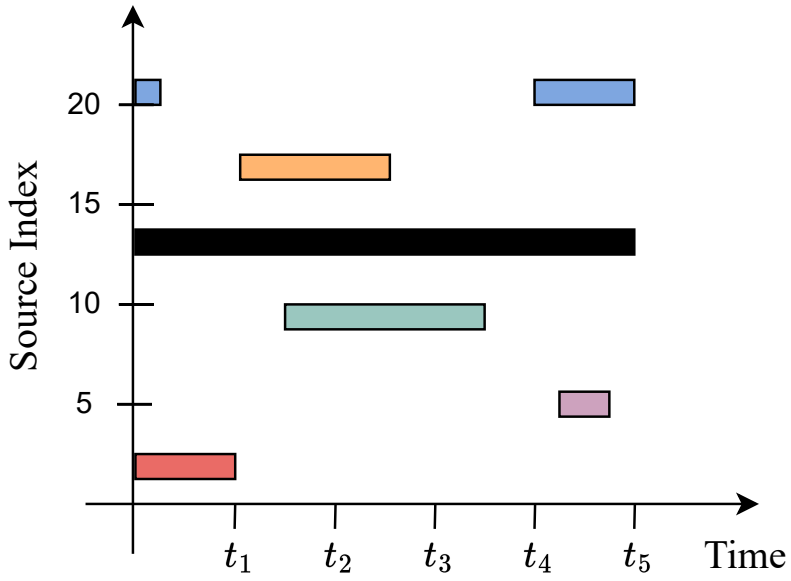

Figure 2.8 Intermittent source activity along with interference. The color filled blocks denote active sources at different time instants. The black block present at all time instants denotes the activity of the interfering jammer.

Assuming synchronized sensors, the signal received at the j-th sensor in the time interval $t_k \leq t < t_{k+1}$ corresponding to the k-th hop (as shown in Figure 2.4) is given by

$$y(j,t) = \sum_{i=1}^{N_k} \left\{ \sqrt{P_i} c_i(t) a^j(\theta_i) \right\} h^t(f_i) + \sqrt{P_{jam}} c_{jam}(t) a^m(\theta_{jam}) h^t(f_{jam}) + w(j,t) \quad (2.5)$$

where, N_k is the number of active sources during the k-th hop ($N_k \ll N$); P_i is the power of the i-th source. The variables $a(\theta_i)$ and $h(f_i)$ are, respectively, the spatial and frequency modes of the i-th source, with $a^j(\cdot)$ and $h^t(\cdot)$ denoting the corresponding j-th and t-th powers; $c_i(t)$ is the complex amplitude of the i-th source. The frequency

mode is given by $h(f_i) = e^{j2\pi f_i}$, with $f_i \in [f_{min}, f_{max}]$ being the carrier frequency of the i-th source during the k-th hop. The hop frequencies are measured relative to the carrier frequency of the receiver. The spatial mode is given by $a(\theta_i) = e^{j2\pi(d/\lambda)\sin(\theta_i)}$, where d/λ is the spacing between antennae expressed in units of wavelength λ, and θ_i is the DOA of the i-th source. P_{jam} is the power of the jammer; c_{jam} denotes the complex amplitude of the jammer; f_{jam} is the constant frequency of the jammer; and θ_{jam} is the DOA of the jammer. $w(j,t)$ is additive zero-mean complex Gaussian noise with variance σ_w^2.

CHAPTER 3

SOURCE PARAMETER AND PATTERN ESTIMATION

The signal model in Equation (2.1) has three sets of unknowns, namely DOAs θ, frequencies f, and complex amplitudes c. Each physical source may emit multiple frequencies as part of a FH pattern, and it may be observed over multiple DOAs for multipath channels. The goal of the process presented in this section is to determine physical sources, and for each physical source to determine an activity pattern and an FH pattern. Two main ideas are that even though a physical source may be observed over many DOAs, the individual DOA activity patterns of a physical source are "similar." DOA information is paired with FH information to associate FH patterns with physical sources. In the following, an approach is proposed that uses the received signal matrix $\mathbf{Y}$ to estimate FH and activity patterns over the course of the observation interval T. This approach includes a FH estimation stage, a DOA estimation stage, hidden state filtering to refine DOA estimates, and a pairing stage that combines information from the previous stages to associated FH patterns with physical sources Figure 3.1 elucidates the relations between the signal processing tasks developed in this section. Each of the processing tasks is detailed next.

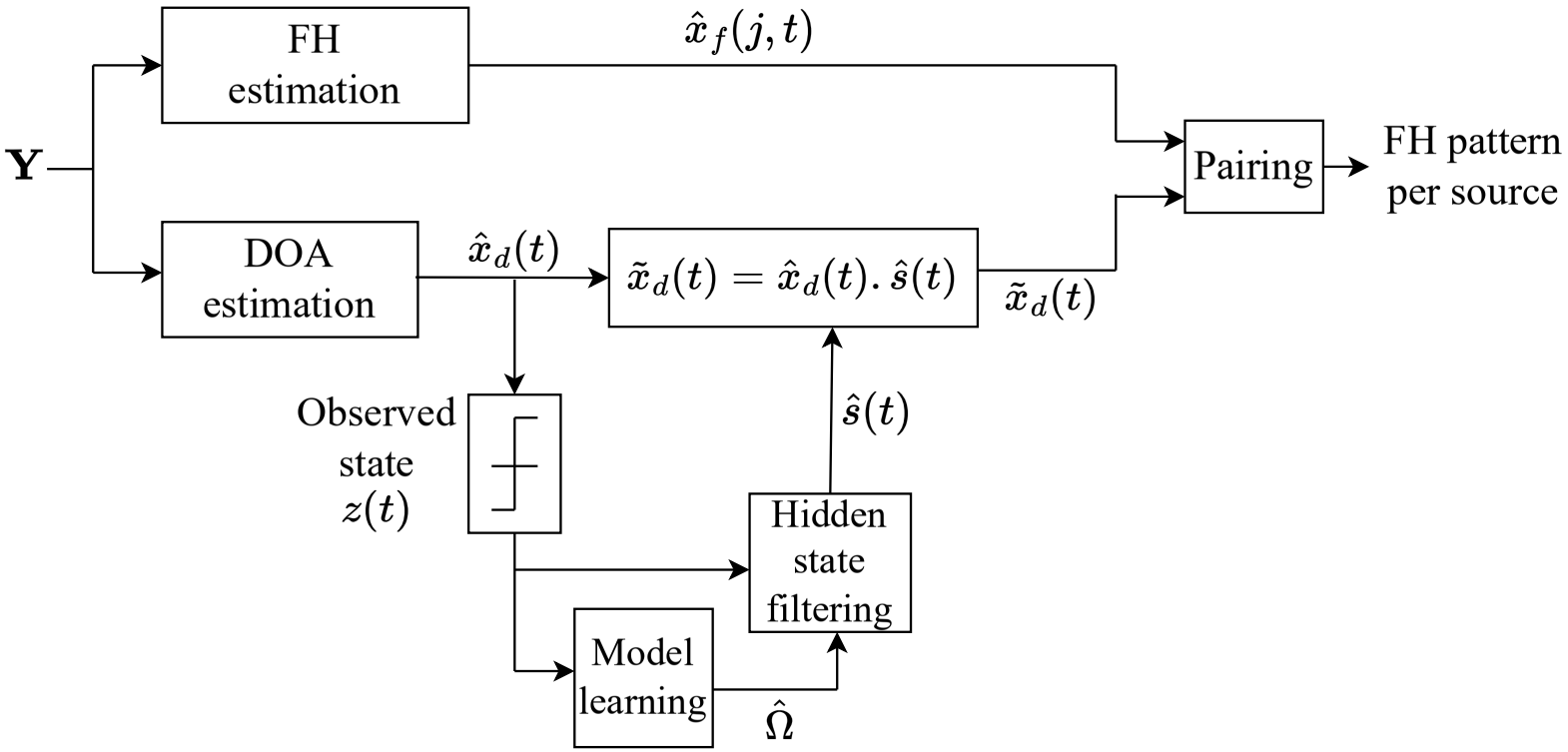

Figure 3.1 Block diagram of the proposed algorithm to separate multiple FH sources and assign source labels.

3.1 FH Estimation

The estimation of the frequency hops at each time instant $0 \leq t \leq T$ is posed as a sparse representation problem. In the following, we define a dictionary matrix, a matrix of unknowns, a measurement matrix, and a noise matrix. For setting up the dictionary, let the set $F = \{f_1, f_2, \ldots, f_{G_f}\}$, with cardinality $G_f \gg N$, comprise all possible hop frequencies f_i. The FH estimation stage samples the frequency by using this grid of frequencies F. The frequency grid is used to define the G_f-length modal vector $\tilde{\mathbf{h}}_f(t)$ at sampling instant t

$$\tilde{\mathbf{h}}_f(t) = [h^t(f_1), h^t(f_2), \ldots, h^t(f_{G_f})] \tag{3.1}$$

Next, this vector is expanded to include all T sampling instants in a TG_f-length vector

$$\mathbf{h}_f(t) = [\underbrace{\mathbf{0}'_{G_f}, \ldots, \mathbf{0}'_{G_f}}_{t}, \tilde{\mathbf{h}}'_f(t), \underbrace{\mathbf{0}'_{G_f}, \ldots, \mathbf{0}_{G_f}}_{T-t-1}]' \tag{3.2}$$

where $\mathbf{0}_{G_f}$ is a vector containing G_f zeros. The FH modal dictionary $\mathbf{H}_f$ is then defined at the $T \times TG_f$ matrix

$$\mathbf{H}_f = [\mathbf{h}_f(1), \mathbf{h}_f(2), \ldots, \mathbf{h}_f(T)]' \tag{3.3}$$

Let $\mathbf{x}_f(j,t)$ be the G_f-length vector of unknown complex amplitudes associated with the grid frequencies at time t and sensor j. This vector is then expanded to form the TG_f-length vector that includes all T time instants

$$\mathbf{x}^*_f(j) = [\mathbf{x}'_f(j,1), \mathbf{x}'_f(j,2), \ldots, \mathbf{x}'_f(j,T)]' \tag{3.4}$$

Across all J sensors and T time instants, the $TG_f \times J$ matrix of complex amplitudes is defined as $\mathbf{X}_f = [\mathbf{x}_f^*(1), \mathbf{x}_f^*(2), \ldots, \mathbf{x}_f^*(J)]$. The solution to the problem being formulated relies on the assumption that the vector $\mathbf{x}(j,t)$ has sparsity. Sparsity entails that the vector $\mathbf{x}(j,t)$ has non-zero entries corresponding only to the active frequencies at each time instant t.

A sparse estimate of the frequency hopping pattern per source $\mathbf{X}_f$ (or equivalently an estimate of $\mathbf{x}_f(j,t)$ for all j and all t) is denoted $\hat{\mathbf{X}}_f$ (or $\hat{\mathbf{x}}_f(j,t)$), and it is found by solving the following optimization problem

$$\hat{\mathbf{X}}_f = \arg\min_{\mathbf{x}_f} \|\mathbf{Y}' - \mathbf{H}_f \mathbf{X}_f\|_2^2 + \lambda_f \sum_{j=1}^{J} \sum_{t=1}^{T} \|\mathbf{x}_f(j,t)\|_1 \tag{3.5}$$

The ℓ_1-norm in Equation (3.5) enforces the sparsity constraint. The hyperparameter λ_f controls the sparsity of the solution. A large λ_f increases the penalty of non-zero elements of $\mathbf{x}_f(j,t)$.

3.2 DOA estimation

To formulate the problem of estimating the DOA of sources at each time instant $0 \leq t \leq T$ as a sparse representation problem, we again define a dictionary matrix and a matrix of unknowns. A grid comprising G_d possible DOAs, $\Theta = [\theta_1, \theta_2, \ldots, \theta_{G_d}]$ is used to define the $J \times G_d$ DOA modal dictionary

$$\mathbf{H}_d = [\mathbf{a}(\theta_1), \mathbf{a}(\theta_2), \ldots, \mathbf{a}(\theta_{G_d})] \tag{3.6}$$

where $\mathbf{a}(\theta_i)$ is the steering vector associated with DOA θ_i defined as $\mathbf{a}(\theta_i) = [1, a(\theta_i), \ldots, a^{M-1}(\theta_i)]'$ (see (Equation 2.1) for other definitions).

Let $\mathbf{x}_d(t)$ be the G_d-length vector of unknown complex amplitudes associated with the grid DOAs at time t. Across all T sampling instants, the $G_d \times T$ matrix of complex amplitudes is defined as $\mathbf{X}_d = [\mathbf{x}_d(1), \mathbf{x}_d(2), \ldots, \mathbf{x}_d(T)]$. Given the observations $\mathbf{Y}$, a sparse estimate of the DOA pattern $\mathbf{X}_d$ (or equivalently an estimate of $\mathbf{x}_d(t)$ for all t) is denoted $\hat{\mathbf{X}}_d$ (or $\hat{\mathbf{x}}_d(t)$), and it is found by solving the following optimization problem

$$\hat{\mathbf{X}}_d = \arg\min_{\mathbf{x}_d} \|\mathbf{Y} - \mathbf{H}_d\mathbf{X}_d\|_2^2 + \lambda_d \sum_{t=1}^{T} \|\mathbf{x}_d(t)\|_1 \tag{3.7}$$

Similar to the optimization problem for estimating the frequency hops, the formulation includes a hyperparameter λ_d that controls sparsity.

3.3 Hidden State Filtering (HSF)

Let $\hat{x}_d(t)$ denote a non-zero component of the solution $\hat{\mathbf{x}}_d(t)$ to the optimization problem in Equation (3.7). Then $\hat{x}_d(t)$ is associated with a single source, and it represents the estimate of the complex amplitude (including the effect of the frequency hop term) of the source at time t. If the state $s(t)$ of the source were known, then $\tilde{x}_d(t) = \hat{x}_d(t) \cdot s(t)$ is a refined estimate of $\hat{x}_d(t)$ in the sense that a spurious component would be removed from the solution to Equation (3.7) if $\hat{x}_d(t) \neq 0$ but $s(t) = 0$. Conversely, the solution would stand if $s(t) = 1$. While the state $s(t)$ is hidden to the observer, it may be inferred from state observations. Let a set $C = \{x | x \neq 0\}$, then an observation $z(t)$ of the state of a source is obtained as $z(t) = 1_C\{\hat{x}_d(t)\}$, where 1_C denotes the indicator function of the set C. Hidden state filtering (HSF) is the problem of inferring a state sequence $s(1:T)$ for each source, given an observation sequence $z(1:T)$ of the source and a HMM model parameter Ω. In the remainder of this subsection, we discuss the forward-backward procedure, which is then used to solve the HSF problem. The algorithms implementing these methods assume that the HMM parameter Ω is known. The estimation of the parameter Ω, when it is not known *a priori*, is addressed in a subsequent subsection.

3.3.1 Forward-Backward procedure

The forward-backward procedure comprises of the iterative calculation of forward and backward variables given the observed state sequence and the model parameter Ω. The forward variable $\alpha_j(t)$ is defined as the probability of a state at time t given the observed state sequence up to and including time t

$$\alpha_j(t) \triangleq P(s(t) = j | z(1:t), \Omega), j = 0, 1 \tag{3.8}$$

Solving for $\alpha_j(t)$ consists of the following steps [50]:

1. Initialization:

$$\alpha_i(1) = \pi_i b_i(z(1)), i = 0, 1 \tag{3.9}$$

2. Induction:

$$\alpha_j(t+1) = \left[\sum_{i \in \{0,1\}} \alpha_i(t) a_{ij} \right] b_j(z(t)),$$
$$j = 0, 1, 0 \leq t \leq T-1 \tag{3.10}$$

3. Termination:

$$P(z(1:T)|\Omega) = \sum_{i=0,1} \alpha_i(T) \tag{3.11}$$

The backward variable $\beta_i(t)$ is defined as the probability of the observation sequence from $t+1$ to the end of the sequence, conditioned on the state $s(t) = i$

$$\beta_i(t) \triangleq P(z(t+1:T) | s(t) = i, \Omega), i = 0, 1 \tag{3.12}$$

Solving for $\beta_i(t)$ consists of the following steps [50]:

1. Initialization:

$$\beta_i(T) = 1, \ i = 0, 1 \tag{3.13}$$

2. Induction:

$$\beta_i(t) = \sum_{j \in \{0,1\}} a_{ij} b_j(z(t+1)) \beta_j(t+1),$$
$$i = 0, 1, t = T-1, T-2, ..., 1 \tag{3.14}$$

Hidden state filtering methods discussed next will use the forward and backward variables.

3.3.2 Individually most probable states

There are different ways of finding the "optimal" state sequence $s(1:T)$ given the observed sequence $z(1:T)$ and the HMM parameter Ω. One reasonable criterion is to choose at each time t, the state that is most probable, given the observed sequence and the HMM parameters. Denote the belief state

$$\gamma_i(t) \triangleq P(s(t) = i | z(1:T), \Omega) \tag{3.15}$$

It can be shown that the variable $\gamma_i(t)$ may be expressed in terms of the forward-backward variables [50]

$$\gamma_i(t) = \frac{\alpha_i(t)\beta_i(t)}{\sum_{j \in \{0,1\}} \alpha_j(t)\beta_j(t)} \tag{3.16}$$

The most probable estimate (MPE) to a state at time t is the solution to the following problem

$$\hat{s}_{\text{MPE}}(t) = \arg\max_{i=0,1} \gamma_i(t) \tag{3.17}$$

Note that the MPE to a state may be computed directly from the forward-backward variables. The MPE state sequence for a source is expressed

$$\hat{s}_{\text{MPE}}(1:T) = \{\hat{s}_{\text{MPE}}(1), \hat{s}_{\text{MPE}}(2), \ldots, \hat{s}_{\text{MPE}}(T)\} \tag{3.18}$$

Using the MPE state sequence, the matrix of complex amplitudes containing the filtered vectors can be calculated as outlined in Algorithm 1.

Algorithm 1. Hidden State Filtering (MPE)

Input: Matrix of complex amplitudes $\hat{\mathbf{X}}_d$ and HMM parameter Ω

Output: Inferred state sequence $\hat{s}_{\text{MPE}}(1:T)$

for each non-zero row of $\hat{\mathbf{X}}_d$ **do**

  for $t = 1:T$ **do**

    $z(t) = 1_c\{\hat{\mathbf{x}}_d(t)\}$

    Calculate $\hat{s}_{\text{MPE}}(t)$ from Equation (3.17).

  end for

end for

3.3.3 Most probable sequence of states

The most probable sequence of states given the observed state sequence of a source is known as the maximum a posteriori (MAP) estimate and is given by

$$\hat{s}_{\text{MAP}}(1:T) = \underset{s(1:T)}{\arg\max} P(s(1:T)|z(1:T)) \tag{3.19}$$

The MAP estimate may be computed using the well-known Viterbi algorithm [51]. The Viterbi algorithm is discussed in detail in Appendix A. The following brief summary of the algorithm follows [50]. Define the quantity

$$\rho_i(t) \triangleq \max_{s(1:t-1)} P(s(1:t-1), s(t) = i|z(1:t), \Omega) \tag{3.20}$$

which represents the joint probability of reaching state i at time t and taking the most probable path. A recursive expression for this probability is obtained noting that if $\rho_i(t-1)$ is known, then $\rho_j(t)$ may be computed by accounting for the transition from state i at time $t-1$ to a state j at time t. This probability may be computed using quantities previously defined according to

$$\rho_j(t) = (\max_i \rho_i(t-1))a_{ij})b_j(z(t)) \tag{3.21}$$

The argument that maximizes Equation (3.21) is denoted as

$$\psi_j(t) \triangleq \arg\max_{i=0,1} (\rho_i(t-1)a_{ij}) \tag{3.22}$$

Following this procedure, the first state that can be determined as part of the most probable path is the final state $s(T)$, since any earlier determination may be affected by later times. This is summarized as follows

1. Initialization:

$$\rho_i(1) = \pi_i b_i(z(1)),\ i = 0, 1 \tag{3.23a}$$

$$\psi_i(1) = 0,\ i = 0, 1 \tag{3.23b}$$

2. Recursion:

$$\rho_j(t) = (\max_i \rho_i(t-1)a_{ij})b_j(z(t)),\ 2 \leq t \leq T,\ j = 0, 1 \tag{3.24a}$$

$$\psi_j(t) \triangleq \arg\max_{i=0,1} (\rho_i(t-1)a_{ij}),\ 2 \leq t \leq T,\ j = 0, 1 \tag{3.24b}$$

3. Termination:

$$\hat{s}_{\text{MAP}}(T) = \arg\max_{i=0,1} (\rho_i(T)) \tag{3.25}$$

4. MAP path:

$$\hat{s}_{\text{MAP}}(t) = \psi_{\hat{s}(t+1)}(t+1),\ t = T-1, T-2, ..., 1 \tag{3.26}$$

Using the MAP path, the matrix of complex amplitudes containing the filtered vectors can be calculated as outlined in Algorithm 2.

Algorithm 2. Hidden State Filtering (MAP)

Input: Matrix of complex amplitudes $\hat{\mathbf{X}}_d$ and HMM parameter Ω
Output: Inferred state sequence $\hat{s}_{\text{MAP}}(1:T)$
for each non-zero row of $\hat{\mathbf{X}}_d$ **do**
    for $t = 1:T$ **do**
        $z(t) = 1_c\{\hat{\mathbf{x}}_d(t)\}$
        Calculate $\hat{s}_{\text{MAP}}(t)$ from Equation (3.26).
    end for
end for

3.3.4 Learning HMM parameters

The HSF methods discussed previously assume the HMM parameter $\Omega = (\mathbf{A}, \mathbf{B}, \pi)$ are known. In practice, however, it cannot be assumed that the model is known in a blind scenario. The goal here is to describe a method by which is estimated based on the observed sequence. Here, the observed sequence refers to the observed activity of sources based on their DOA estimates. The HMM parameters are learnt from the observed sequences of the sources deemed active by the DOA estimation step according to $\hat{\Omega} = \arg\max_{\Omega} P(z(1:T|\Omega)$. For the first (estimated) active source, the HMM parameter $\Omega = (\mathbf{A}, \mathbf{B}, \pi)$ are randomly initialized. For the subsequent estimated sources, the initial parameter is the Ω obtained from the previously estimated active source. The parameter obtained from the last active source is then used to calculate the hidden state sequences using the MPE and MAP methods. For the purpose of estimating the HMM parameter Ω, the following quantity is defined

$$\xi_{i,j}(t) = P(s(t) = i, s(t+1) = j|z(1:T), \Omega) \tag{3.27}$$

It can be shown that the variable $\xi_{i,j}(t)$ may be expressed in terms of the forward-backward variables [50]

$$\xi_{i,j}(t) = \frac{\alpha_i(t) a_{ij} b_j(\hat{z}(t+1)) \beta_j(t+1)}{\sum_{i=0,1} \sum_{j=0,1} \alpha_i(t) a_{ij} b_j(z(t+1)) \beta_j(t+1)} \tag{3.28}$$

Utilizing the forward variable $\alpha_j(t)$ defined in Equation (3.8), the backward variable $\beta_i(t)$ defined in Equation (3.12), the belief state $\gamma_i(t)$ defined in Equation (3.15) and the quantity $\xi_{i,j}(t)$ defined in Equation (3.27) , the HMM parameters are learnt in the following steps:

1. Initialization: Randomly initialize $\Omega = (\mathbf{A}, \mathbf{B}, \pi)$ for the first active source.

2. For each source deemed active by the DOA estimation step:

   (a) Use Equations (3.9) - (3.11) to calculate $\alpha_j(t)$ and Equations (3.13) - (3.14) to calculate $\beta_i(t)$.

   (b) Use Equation (3.16) to calculate $\gamma_i(t)$ and Equation (3.28) to calculate $\xi_{i,j}(t)$.

   (c) Update model parameters:

$$\hat{\pi}_i = \gamma_i(1) \tag{3.29a}$$

$$\hat{a}_{ij} = \frac{\sum_{t=1}^{T-1} \xi_{i,j}(t)}{\sum_{t=1}^{T-1} \gamma_i(t)} \tag{3.29b}$$

$$\hat{b}_j(k) = \frac{\sum_{t=1}^{T} \mathbf{1}(z(t) = k)\gamma_j(t)}{\sum_{t=1}^{T} \gamma_j(t)} \tag{3.29c}$$

   Here $\mathbf{1}(a)$ is the indicator function, i.e., $\mathbf{1}(a) = 1$ if a is true and 0 otherwise.

   (d) Set $\hat{\Omega} = (\hat{\mathbf{A}}, \hat{\mathbf{B}}, \hat{\pi})$, and repeat step (2).

The last HMM parameters $\hat{\Omega} = (\hat{\mathbf{A}}, \hat{\mathbf{B}}, \hat{\pi})$ obtained after running through the observed state sequence of all sources is considered as the common model for all sources. The HMM parameter learning is outlined in Algorithm 3.

Algorithm 3. Learning HMM parameters

Input: Matrix of complex amplitudes $\hat{\mathbf{X}}_d$

Output: Learnt HMM parameters $\hat{\Omega} = (\hat{\mathbf{A}}, \hat{\mathbf{B}}, \hat{\pi})$

Initialize $\Omega = (\mathbf{A}, \mathbf{B}, \pi)$.

for each non-zero row of $\hat{\mathbf{X}}_d$ **do**

  for $T = 1 : t$ **do**

    $z(t) = 1_c\{\hat{\mathbf{x}}_d(t)\}$

    while no convergence **do**

      Obtain $\alpha_j(t)$ and $\beta_i(t)$ using Forward-Backward procedure

      Update $\hat{\Omega} = (\hat{\mathbf{A}}, \hat{\mathbf{B}}, \hat{\pi})$ using Equations (3.29a)-(3.29c)

    end while

    $\Omega \leftarrow \hat{\Omega}$.

  end for

end for

3.4 Pairing

Given the FH and DOA estimates, the final stage is to pair them. The goal is not to physically localize the sources (or clusters), but to associate a DOA pattern with a FH pattern. For each time instant t, the pairing stage is designed to pick a combination of DOA and FH estimates that provide the best fit to the observed data.

To perform the pairing, two new dictionaries $\tilde{\mathbf{H}}_d$ and $\tilde{\mathbf{H}}_f$ are formed from the original respective dictionaries $\mathbf{H}_d$ and $\mathbf{H}_f$. The new dictionary $\tilde{\mathbf{H}}_d$ is defined as a submatrix of $\mathbf{H}_d$, with elements corresponding to non-zero entries in $\hat{\mathbf{X}}_d$. Similarly, the new dictionary $\tilde{\mathbf{H}}_f$ is defined as a submatrix of $\mathbf{H}_f$, with elements corresponding to non-zero entries in $\hat{\mathbf{X}}_f$. The new dictionaries are introduced to limit the computational cost of the pairing operation, and used to create a new dictionary [52]. The Kronecker product of $\tilde{\mathbf{H}}_d$ and $\tilde{\mathbf{H}}_f$ defines this new dictionary $\tilde{\mathbf{H}}$

$$\tilde{\mathbf{H}} = \tilde{\mathbf{H}}_d \otimes \tilde{\mathbf{H}}_f \tag{3.30}$$

This dictionary is a grid that contains all active frequencies for each active DOA over the entire period of observation, after the activity of secondary sources has been removed. The pairing stage utilizes this newly formed dictionary of frequencies and DOAs $\tilde{\mathbf{H}}$ to estimate the matrix $\mathbf{X}$, which contains the complex amplitudes of sources which are indexed by their hop frequencies and their DOAs. The following optimization problem is solved

$$\hat{\mathbf{X}} = \arg\min_{\mathbf{x}} \|\mathbf{Y} - \tilde{\mathbf{H}}\mathbf{X}\|_2^2 + \lambda \sum_{t=1}^{T} \|\mathbf{x}(t)\|_1 \tag{3.31}$$

to obtain a sparse vector $\mathbf{x}(t)$ whose non-zero elements are the estimated complex amplitudes. Here λ is the hyperparameter that controls the sparsity of $\mathbf{x}(t)$. The pairing of FH estimates and DOA is outlined in Algorithm 4.

Algorithm 4. Pairing of DOA and FH estimates

1: **Input:** Matrices of complex amplitudes $\hat{\mathbf{X}}_d$, $\hat{\mathbf{X}}_f$ and dictionaries $\mathbf{H}_d$, $\mathbf{H}_f$

2: **Output:** Matrix of paired DOA and FH estimates $\hat{\mathbf{X}}$

3: Obtain new dictionary $\tilde{\mathbf{H}}_d$ from $\mathbf{H}_d$

4: Obtain new dictionary $\tilde{\mathbf{H}}_f$ from $\mathbf{H}_f$

5: Create dictionary $\tilde{\mathbf{H}}$ using Equation (3.30)

6: Obtain $\hat{\mathbf{X}}$ from Equation (3.31)

Source separation is obtained by labeling the sources according to DOA estimates. A source label may be associated with multiple frequency hops. Furthermore, the pairing stage is also capable of reducing false alarms in the FH and DOA estimation stages by allowing only solutions for which a source is active at a given time instant only if produces a joint FH and DOA estimate.

CHAPTER 4

NUMERICAL RESULTS

In this section, numerical results are presented to demonstrate the performance of the proposed approach to separate intermittent FH signals. We assume that the activity for each source is defined by an HMM with transition probabilities $a_{01} = 0.02$ and $a_{10} = 0.02$. A modal dictionary for DOA estimation is considered with $G_d = 36$ bins, each having a bin size of 5 degrees. The FH grid has $G_f = 40$ bins with a spacing of 50 kHz for a 2 MHz total bandwidth. The signals being transmitted are slow FH signals in which each hop contains one or more symbols. Frequency hops do not violate the narrowband assumption for DOA estimation. The number of unresolveable multipaths per cluster is set as $M = 20$ and the deviation from mean DOA of each cluster has a variance of $\sigma_\theta^2 = 2$ degrees [15–17]. In the following figures, we consider two clusters per source while referring to multiple-cluster sources.

Figures 4.1 and 4.2 provide illustrative examples for the LOS propagation environment. Figure 4.1 shows the true and estimated FH activity for two sources for $M = 10$ sensors. Without the pairing stage, FH signals cannot be assigned source labels. In such a case, each hop is treated as a distinct source and thus, the FH estimation stage estimates five sources over the period of observation.

Figure 4.2 shows the true and estimated DOAs of two LOS sources with intermittent activity. Figure 4.2(a) shows the DOA vs. time for the two sources. Figure 4.2(b) shows the DOA estimates vs. time with no HSF. Many false alarms are apparent. Figures 4.2(c) and 4.2(d) illustrate the ability of HSF in the form of MPE and MAP filtering, respectively, to reduce false alarms.

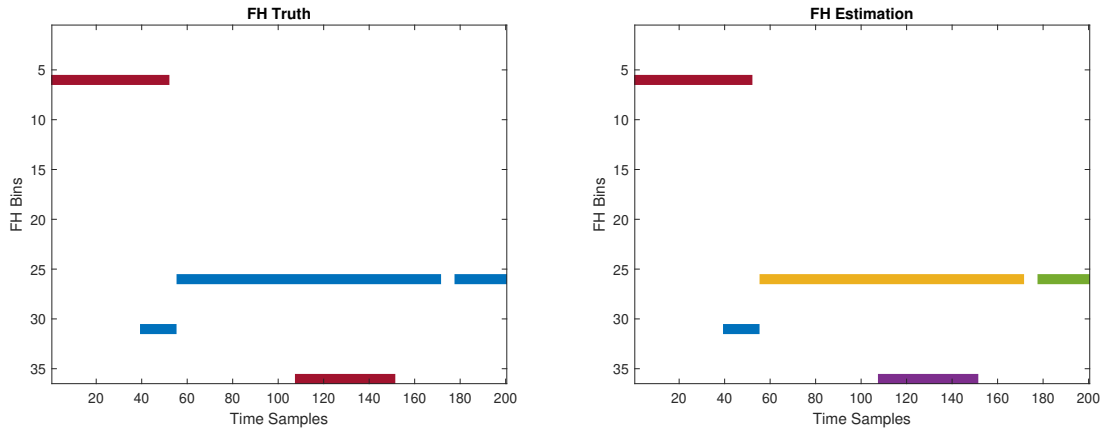

(a) FH Truth **(b)** FH Estimation

Figure 4.1 FH truth and estimation for two sources. ($M = 10$ sensors).

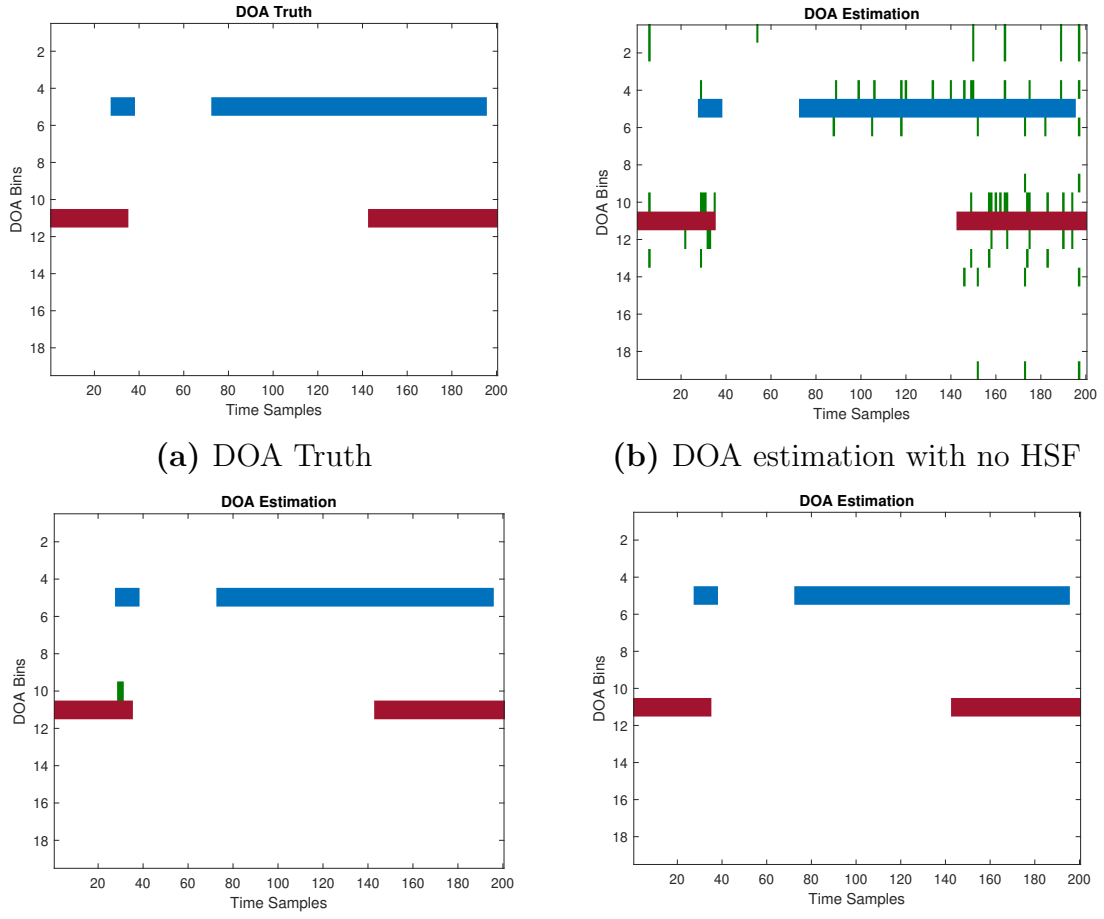

(a) DOA Truth **(b)** DOA estimation with no HSF

(c) DOA estimation with HSF (MPE) **(d)** DOA estimation with HSF (MAP)

Figure 4.2 True DOA activity and estimation for two LOS sources with intermittent source activity. ($M = 10$ sensors).

The performance criterion chosen is the receiver operating characteristic (ROC), in which the probability of correct detection P_d is plotted against the probability of false alarm P_{fa}. The probability of correct detection for source activity is computed as the ratio of the number of correctly detected sources to the number of true active sources. A source activity is deemed a correct detection if it has a "similar" source activity over the total observation interval as a true active source. Multiple activity patterns associated with different DOAs are considered "similar" if they match over a prescribed fraction, ϱ, of the time samples at which their values are 1. Through experimentation, this fraction is chosen to be $\varrho = 0.95$. The probability of false alarm for source activity is the ratio of the number of spuriously detected sources over the entire observation interval to the number of true active sources. A source activity is spurious if a source is detected to be active when no true source is active. Analogous definitions apply to P_d and P_{fa} of frequency hops and to paired activity.

Figure 4.3 shows the ROC of FH estimation for five sources with an SNR per source of 10 dB. For $P_{fa} = 0.3$, the FH estimation has $P_d = 0.98$. The performance of the FH estimation affects the source separation, as the pairing uses the estimations from both the previous stages to pick a pair of DOA and FH pattern that best fits the received signals at each time instant. This is demonstrated later, in the ROC of paired activity.

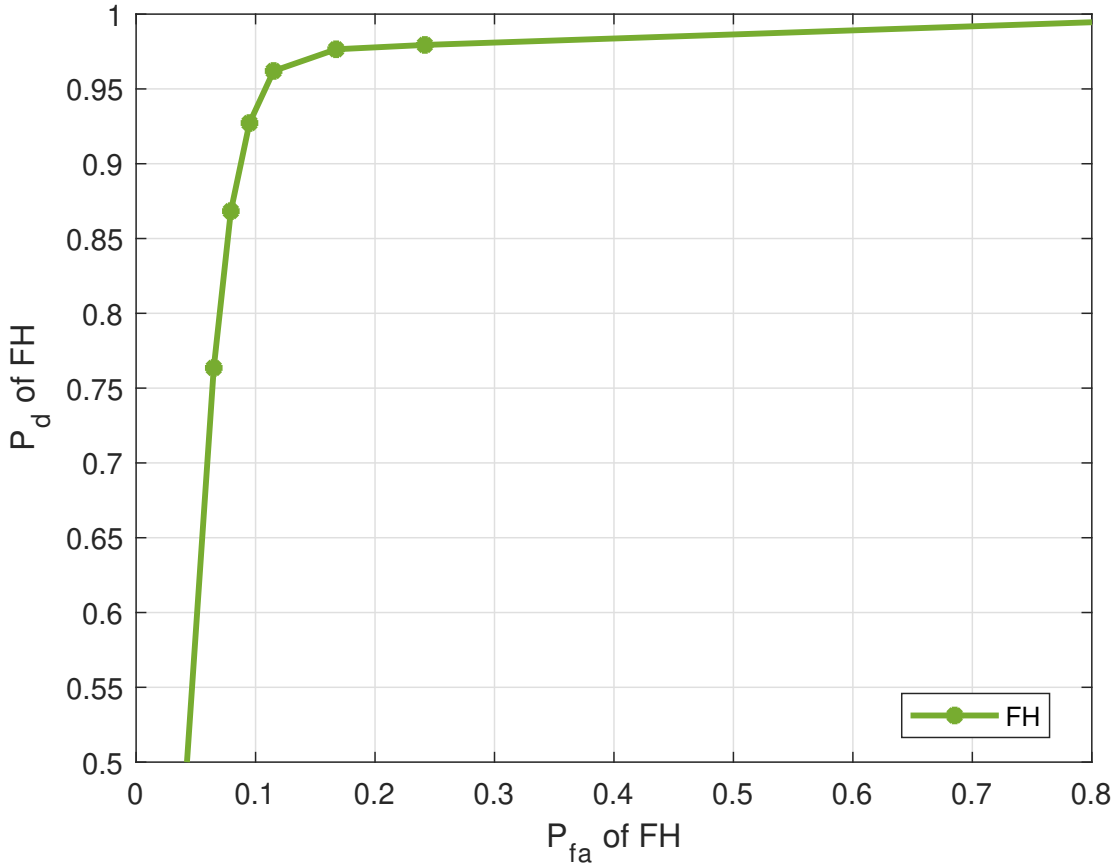

Figure 4.3 P_d versus P_{fa} of FH estimates (5 sources, $J = 20$ sensors, $T = 1000$ samples, SNR = 10 dB).

Figure 4.4 demonstrates the effect of HSF on the correct detection of activity for five LOS sources with an SNR per source of 10 dB. The figure shows the ROC performance with two HSF techniques. The ROC is obtained by solving Equation (3.7), followed by thresholding of $\hat{\mathbf{X}}_d$.The threshold ranges from the smallest to the largest values in the matrix $\hat{\mathbf{X}}_d$ obtained by solving Equation (3.7). Each point of the ROC, consisting of a pair of probability of correct detection and probability of false alarm, corresponds to one of these threshold values. Without filtering, for P_{fa} of activity = 0.3, P_d of activity = 0.67. For the same P_{fa}, with MPE applied, $P_d = 0.86$ when Ω is learnt, and $P_d = 0.87$ when Ω is known. With MAP applied, $P_d = 0.96$ when Ω is learnt, and $P_d = 0.97$ when Ω is known.

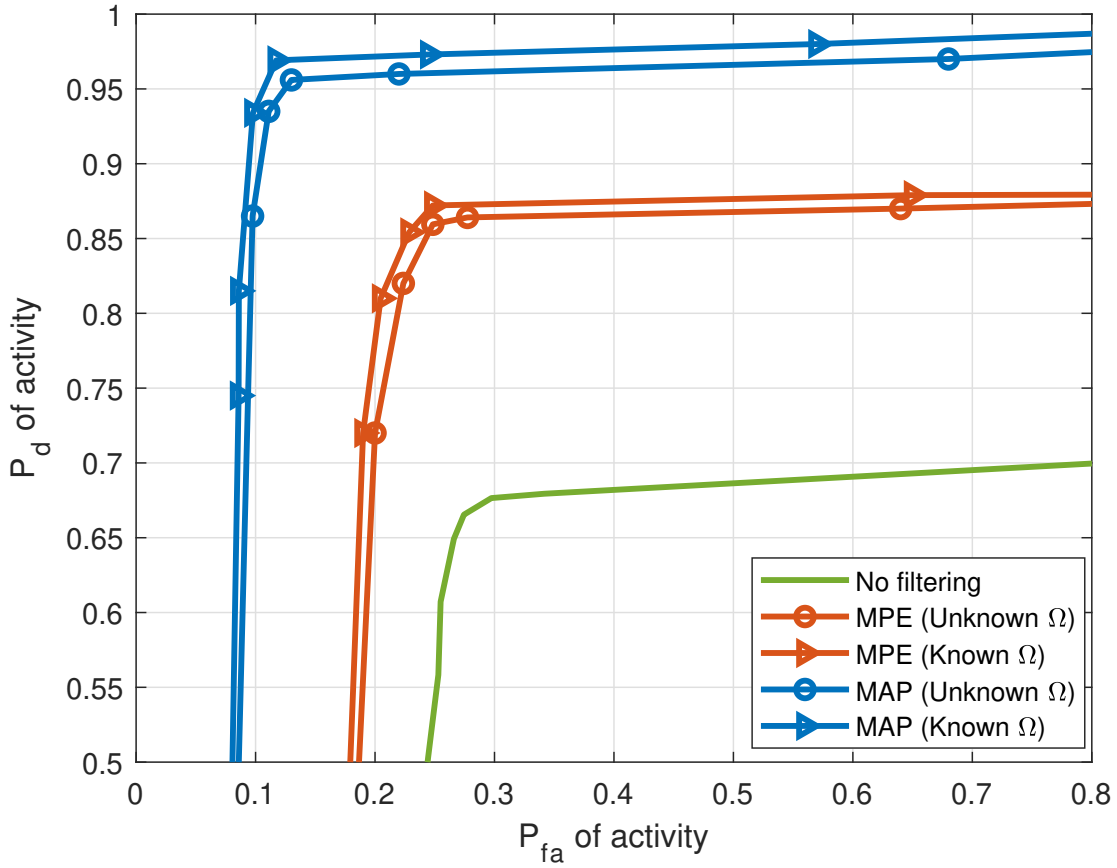

Figure 4.4 P_d versus P_{fa} of activity with and without HSF for LOS propagation environment (5 sources, $J = 20$ sensors, $T = 1000$ samples, SNR = 10 dB).

Figure 4.5 compares the performance for a source in the presence of stronger sources. The one weak source has a SNR = 5 dB and the remaining four sources have a SNR = 10 dB. The figure shows the ROC performance with two HSF techniques, MAP and MPE with unknown Ω. The ROC is again obtained by solving Equation (3.7), followed by thresholding of $\hat{\mathbf{X}}_d$.The threshold ranges from the smallest to the largest values in the matrix $\hat{\mathbf{X}}_d$ obtained by solving Equation (3.7). This ROC demonstrates that as expected there is some degradation in performance, but that the proposed approach can still provide reliable source separation.

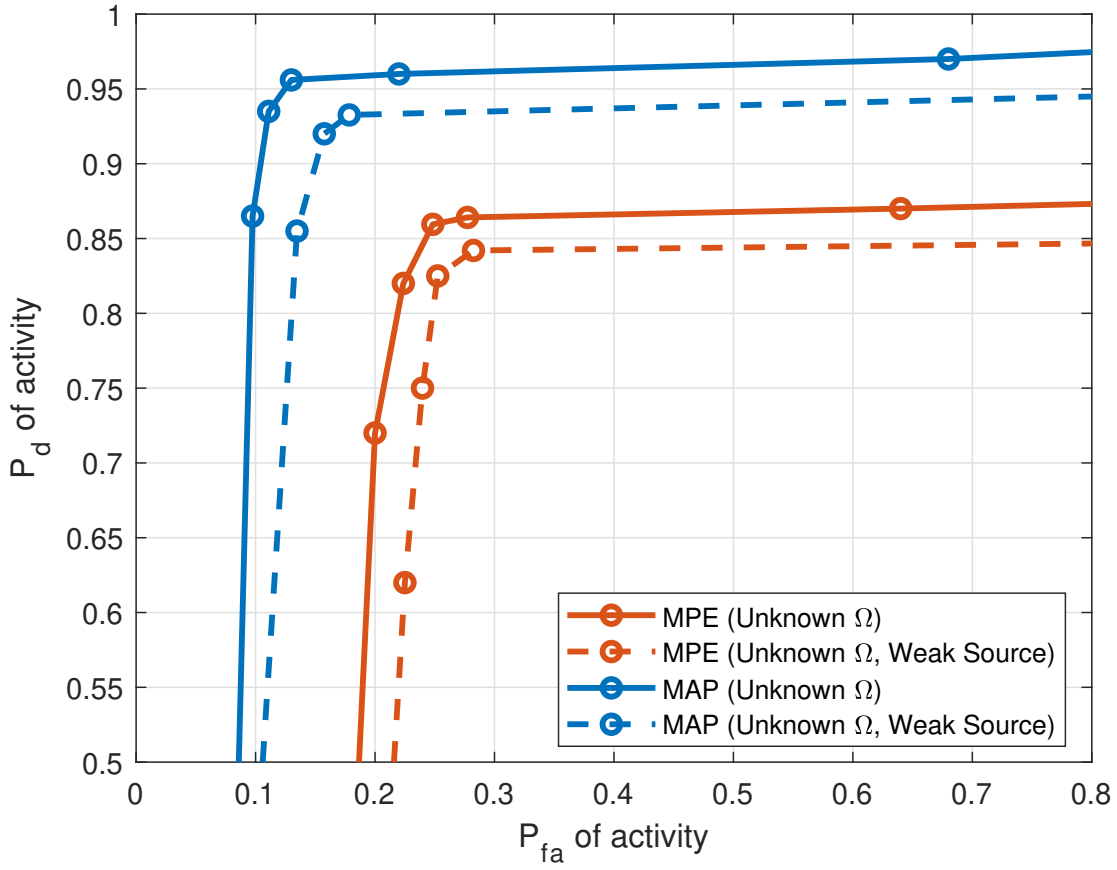

Figure 4.5 P_d versus P_{fa} of activity in presence of stronger sources for LOS propagation environment (5 sources, $J = 20$ sensors, $T = 1000$ samples).

Figure 4.6 demonstrate the effect of HSF on the correct detection of activity for five single-cluster sources. The same improvement in performance is observed in all cases when HSF is applied. Without filtering, for P_{fa} of activity $= 0.6$, P_d of activity $= 0.63$. For the same P_{fa}, with MPE applied after activity estimation, $P_d = 0.76$ when Ω is learnt, and $P_d = 0.78$ when Ω is known. With MAP applied, $P_d = 0.85$ when Ω is learnt, and $P_d = 0.87$ when Ω is known.

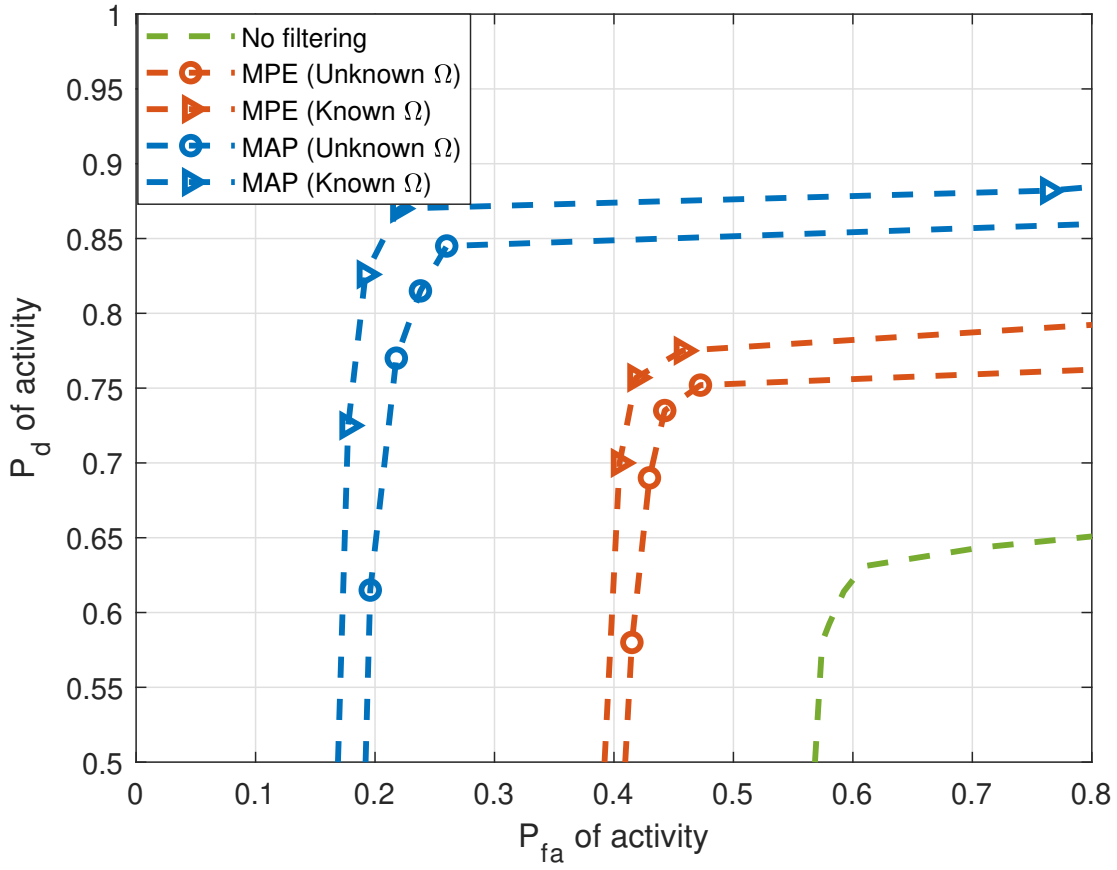

Figure 4.6 P_d versus P_{fa} of activity with and without HSF for single-cluster propagation environment (5 sources, $J = 20$ sensors, $T = 1000$ samples, SNR = 10 dB).

Figure 4.7 demonstrates the effect of HSF on the correct detection of activity for five multiple-cluster sources for $\varrho = 1$. Similarly, Figures 4.9 and 4.8 demonstrate the effect of HSF on the correct detection of activity for five multiple-cluster sources for $\varrho = 0.95$ and $\varrho = 0.9$, respectively. Based on the value of the fraction ϱ chosen to measure similarity of activity patterns, difference in performance is observed. When selection of ϱ is too strict (as in Figure 4.7), changes in activity due to multipath causes the algorithm to not identify clusters from the same source. On the other hand, when selection of ϱ is too relaxed (as in Figure 4.8), activity patterns of clusters of different sources are deemed "similar", which causes deterioration in performance. Based on

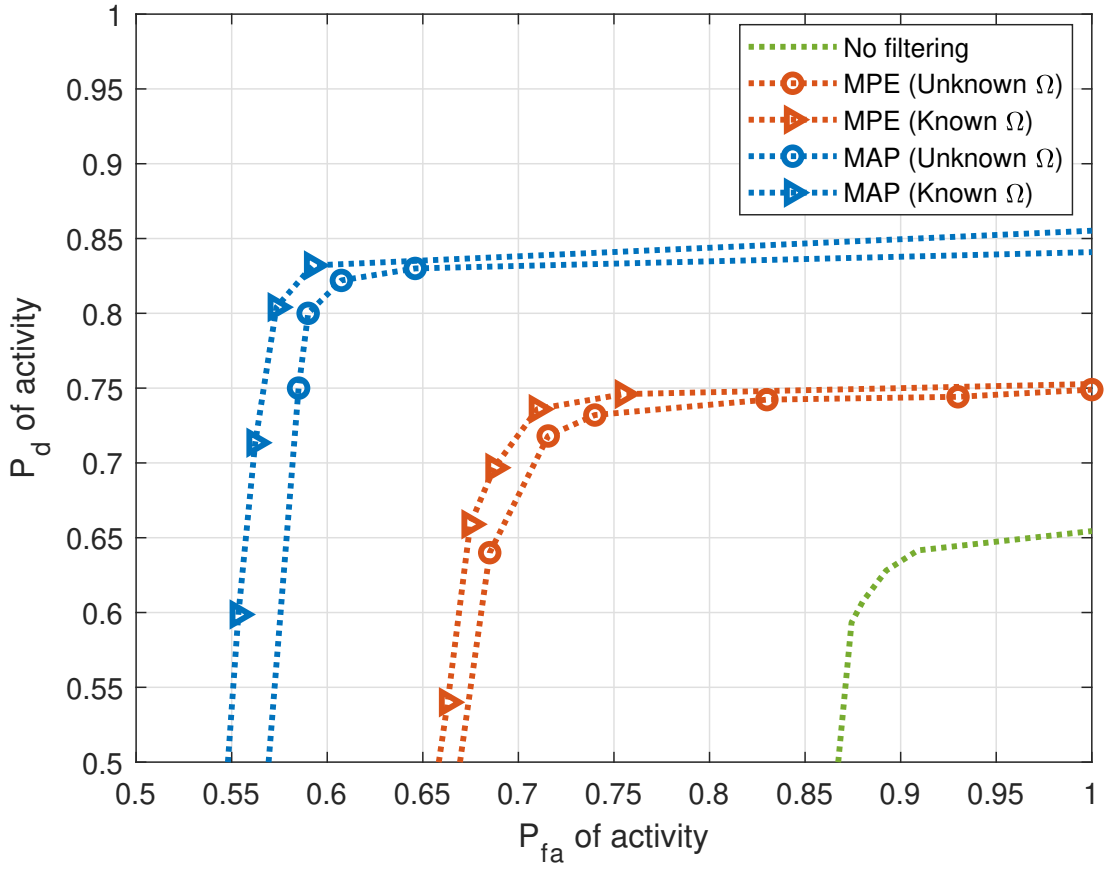

Figure 4.7 P_d versus P_{fa} of activity with and without HSF for 2-cluster propagation environment (5 sources, $J = 20$ sensors, $T = 1000$ samples, SNR $= 10$ dB, $\varrho = 1$).

source signal models, in our case, $\varrho = 0.95$ is the best choice. Also, improvement in performance is observed in all cases when HSF is applied. For $P_{fa} = 0.9$, with MPE applied after activity estimation, $P_d = 0.74$ when Ω is learnt, and $P_d = 0.75$ when Ω is known. With MAP applied, $P_d = 0.84$ when Ω is learnt, and $P_d = 0.85$ when Ω is known.

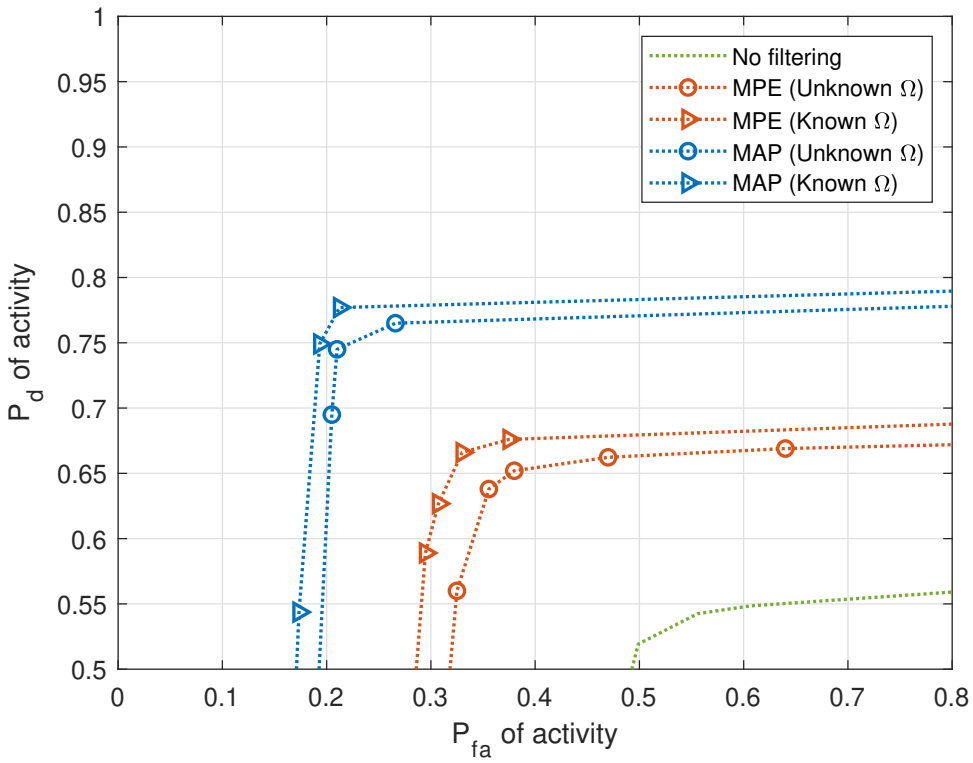

Figure 4.8 P_d versus P_{fa} of activity with and without HSF for 2-cluster propagation environment (5 sources, $J = 20$ sensors, $T = 1000$ samples, SNR $= 10$ dB, $\varrho = 0.9$).

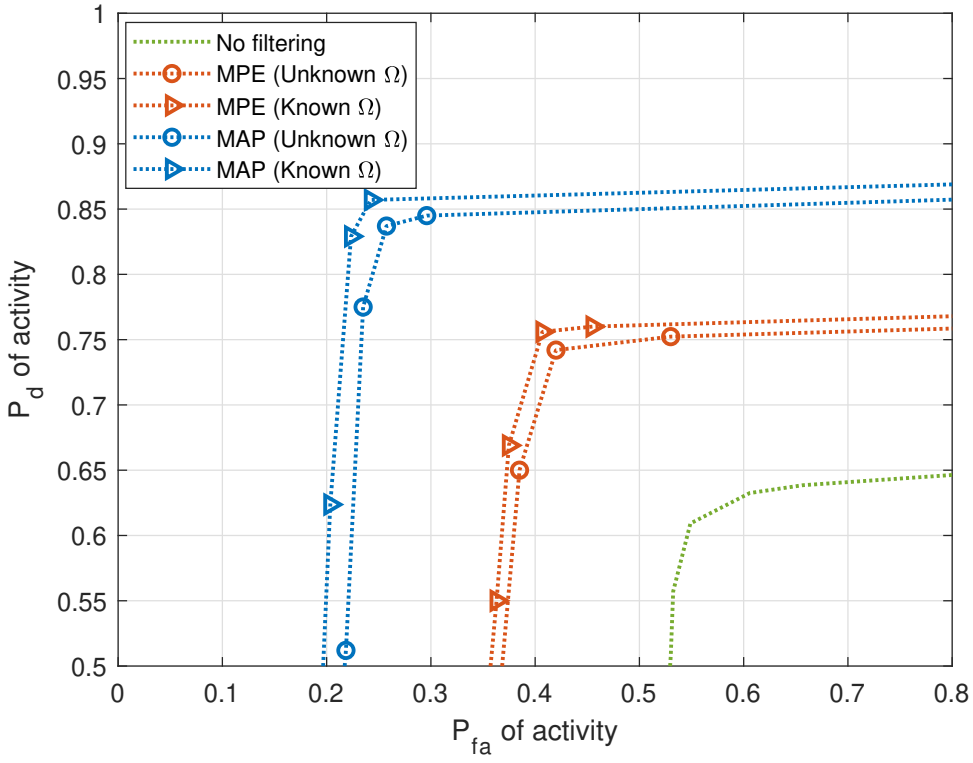

Figure 4.9 P_d versus P_{fa} of activity with and without HSF for 2-cluster propagation environment (5 sources, $J = 20$ sensors, $T = 1000$ samples, SNR $= 10$ dB, $\varrho = 0.95$).

Figure 4.10 shows the ROCs of paired activity for LOS, single-cluster and multiple-cluster propagation environments. In this case, ROC is obtained by solving Equation (3.7) followed by thresholding of $\hat{\mathbf{X}}$. For performance of pairing activity, $\varrho = 0.95$ is used. For a probability of false alarm $P_{fa} = 0.6$, the probability of correct detection of a paired activity with MAP is $P_d = 0.81$ and with MPE $P_d = 0.7$ for multiple-cluster sources. For a probability of false alarm $P_{fa} = 0.6$, the probability of correct detection of a paired activity with MAP is $P_d = 0.84$ and with MPE $P_d = 0.74$ for single-cluster sources. For a probability of false alarm $P_{fa} = 0.6$, the probability of correct detection of a paired activity with MAP is $P_d = 0.95$ and with MPE $P_d = 0.86$ for LOS propagation environment.

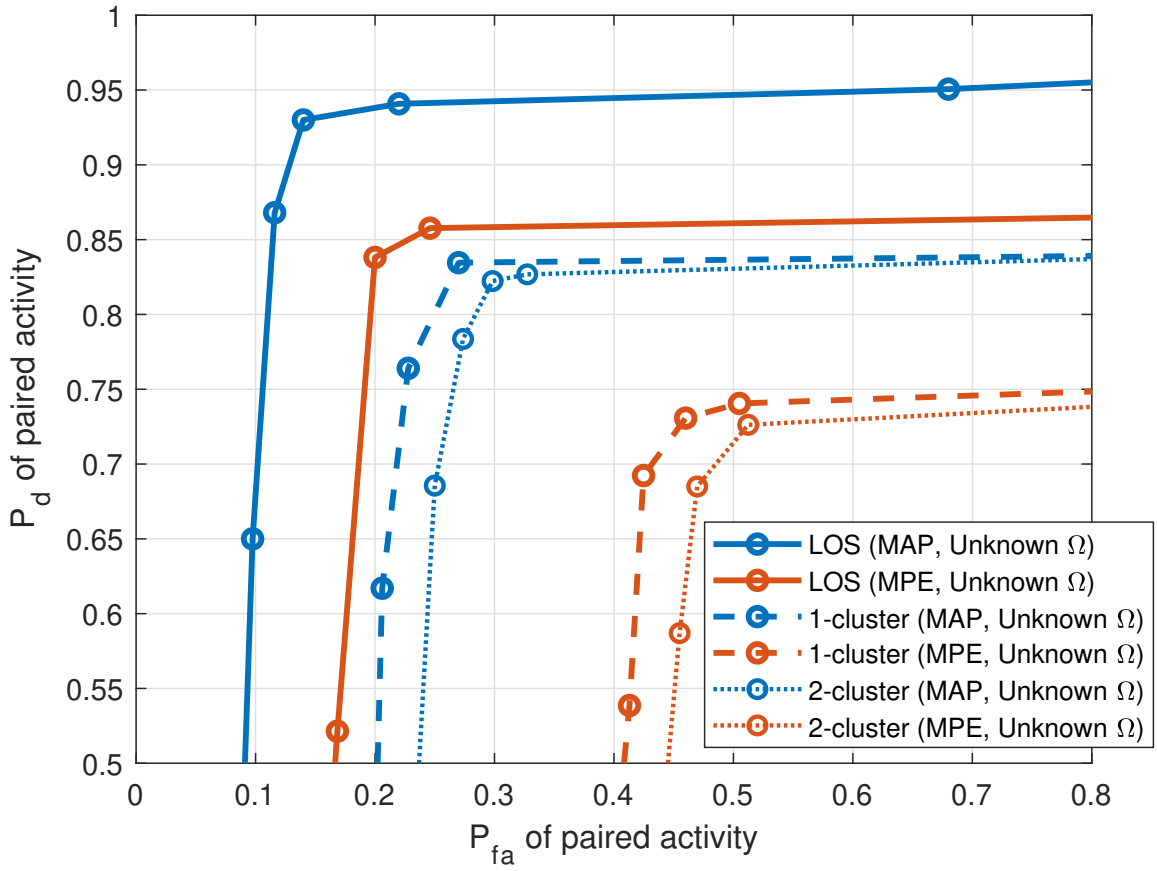

Figure 4.10 P_d versus P_{fa} of paired activity with and without HSF (5 sources, $J = 20$ sensors, $T = 1000$ samples, SNR $= 10$ dB, $\varrho = 0.95$).

Figure 4.11 plots the probability of detection as a function of the number of sources that are present during the period of observation of $T = 1000$ samples. The sources are observed at an SNR per source of 10 dB, and have angular spread of variance $\sigma_\theta^2 = 2$. The detection threshold was set at a probability of false alarm $P_{fa} = 0.15$. Pairing combined with HSF demonstrates its robustness to the mutual interference between sources by showing the slowest decrease of P_d as a function of the number of sources.

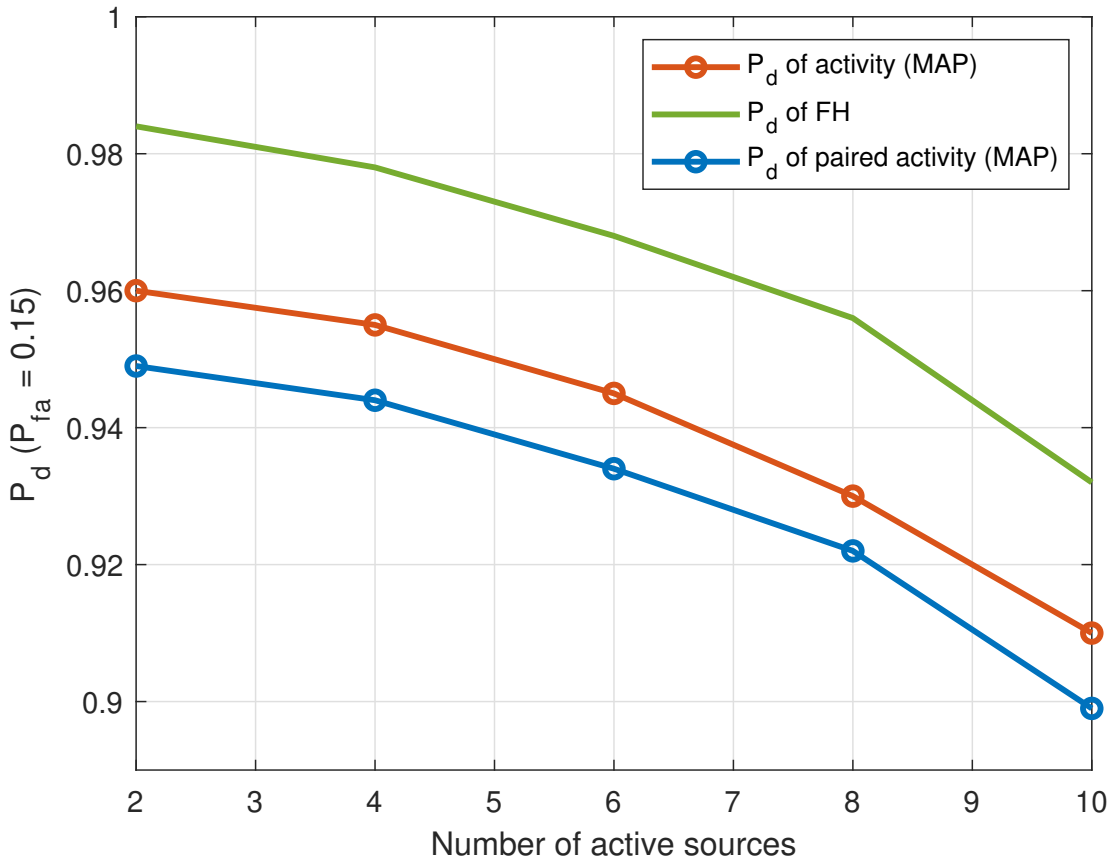

Figure 4.11 P_d when $P_{fa} = 0.15$ versus number of intermittent sources detected active during observation interval in the LOS propagation environment ($J = 20$ sensors, $T = 1000$ samples, SNR = 10 dB).

Figure 4.12 demonstrates the effect of HSF on the correct detection of 5 intermittent sources of interest with an SNR per source of 10 dB; and a jammer that is active at all time instants with an SNR of 20 dB. Without filtering, for a probability of false alarm $P_{fa} = 0.75$, the probability of correct detection is $P_d = 0.64$. For the sameP_{fa}, with MPE applied, $P_d = 0.82$ when Ω is learnt, and $P_d = 0.84$ when Ω is known. With MAP applied, $P_d = 0.94$ when Ω is learnt, and $P_d = 0.95$ when Ω is known. The results demonstrate that HMM parameter learning is very efficient. MAP with learnt HMM parameter Ω performs almost similarly to the case where Ω is known.

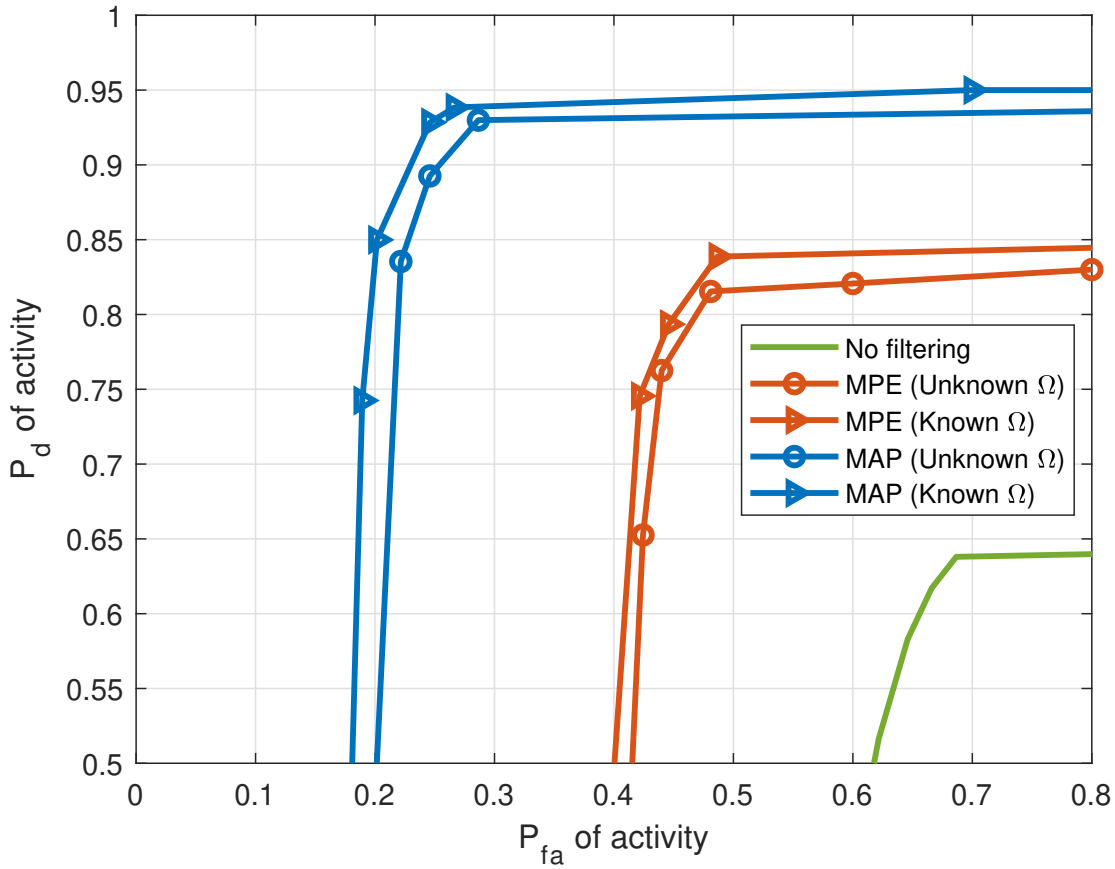

Figure 4.12 P_d versus P_{fa} for activity for LOS propagation environment with interference with and without HSF (5 intermittent sources with SNR = 10 dB, 1 jammer with SNR = 20 dB, $J = 20$ sensors, $T = 1000$ samples).

The ratio of the jammer power to the power of the intermittent sources of interest is referred to as Jammer to Signal Ratio (JSR). Figure 4.13 plots the probability of false alarm as a function of JSR of the sources. As JSR increases, the power of the jammer increases relative to the sources' power. This causes the accuracy of the activity estimates, and therefore source separation, to degrade. It is observed that applying the HSF techniques improve source separation and probability of false alarm reduces for the same JSR. This reduces the effect of the interference on the source separation problem. It is also observed that MAP outperforms MPE, for both known and unknown HMM parameter Ω.

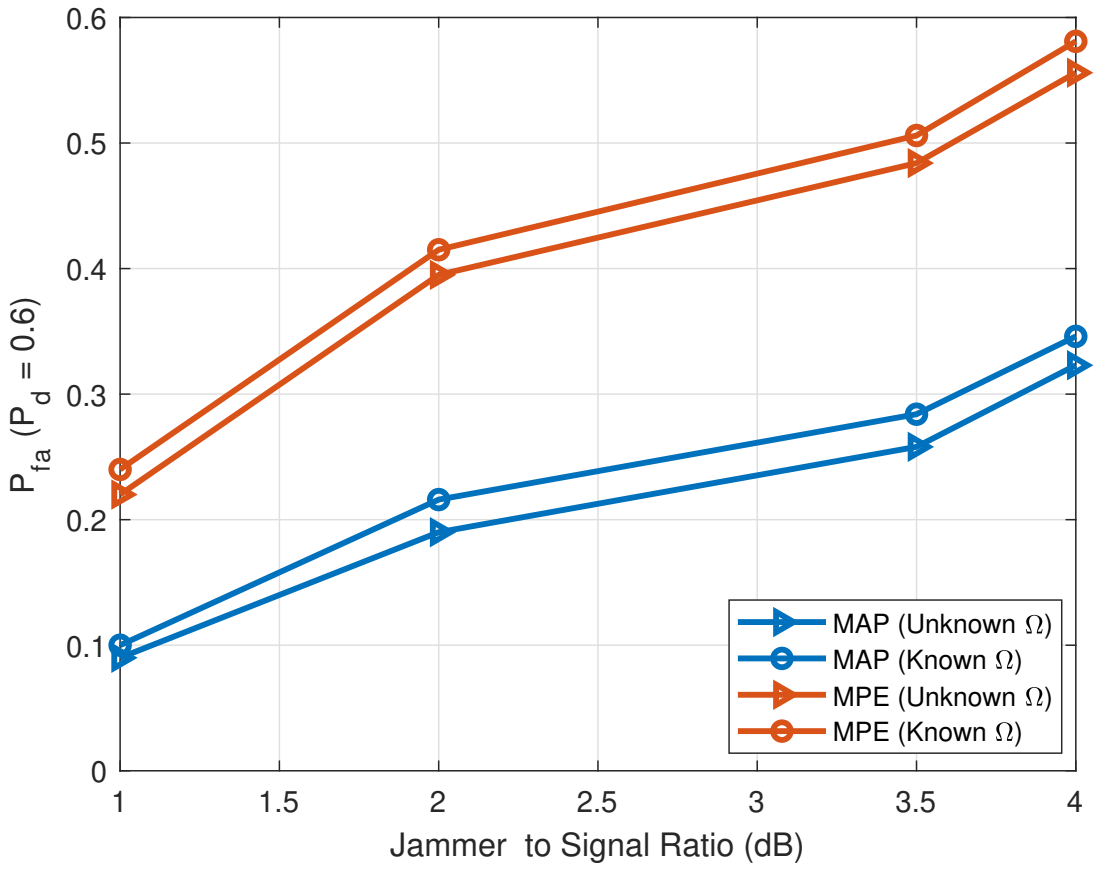

Figure 4.13 P_{fa} of activity when $P_{fa} = 0.6$ versus Jammer to Signal Ratio in dB (5 intermittent sources with SNR = 10 dB, 1 jammer, $J = 20$ sensors, $T = 1000$ samples).

Figure 4.14 plots ROCs for correct detection of paired activity for the same scenario as in Figure 4.12. Without filtering, for a probability of false alarm $P_{fa} = 0.75$ the probability of correct detection is $P_d = 0.63$. For the same P_{fa}, with MPE applied after activity estimation, $P_d = 0.81$ when Ω is learnt, and $P_d = 0.83$ when Ω is known. With MAP applied, $P_d = 0.91$ when Ω is learnt, and $P_d = 0.93$ when Ω is known. The performance of both MAP and MPE filtering is implemented with learnt Ω. For all propagation environments, it is observed that MAP filtering outperforms MPE filtering.

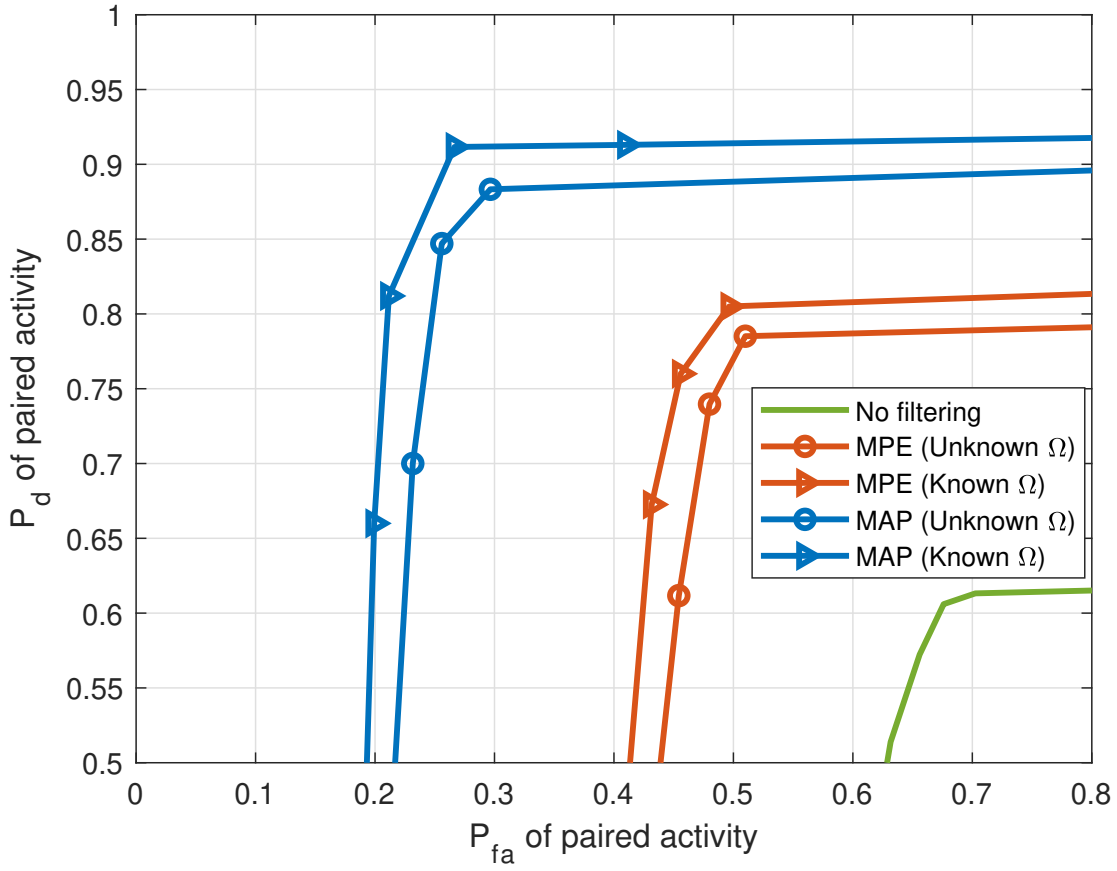

Figure 4.14 P_d versus P_{fa} for activity (5 intermittent sources with SNR = 10 dB, 1 jammer with SNR = 20 dB, $J = 20$ sensors, $T = 1000$ samples).

Figure 4.15 plots the probability of correct detection as a function of the number of intermittent sources of interest present during the period of observation of $T = 1000$ samples. The sources of interest are observed at an SNR per source of 10 dB; and the jammer has an SNR = 20 dB. It is observed that the source separation performance is dependant on the performance of the individual FH and DOA estimation steps.

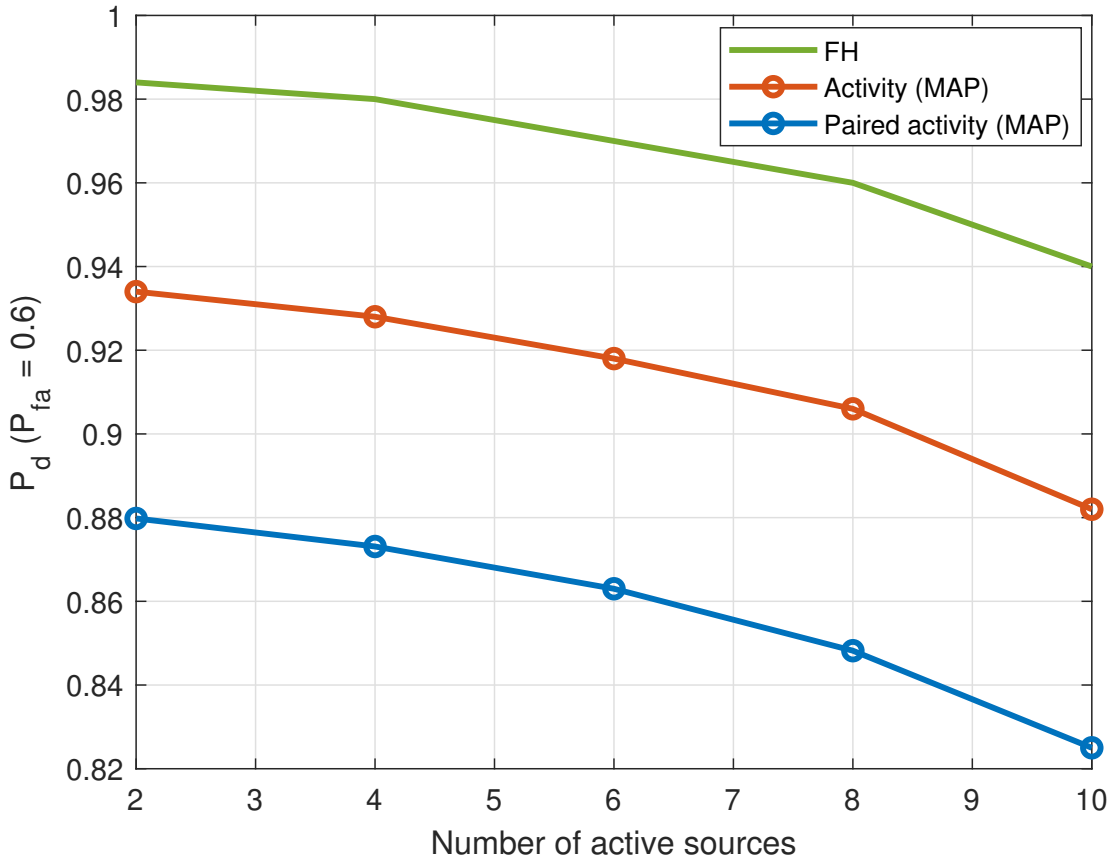

Figure 4.15 P_d when $P_{fa} = 0.6$ versus number of intermittent sources detected active in LOS propagation environment with interference ($J = 20$ sensors, $T = 1000$ samples, SNR of jammer = 20 dB, SNR of sources = 10 dB).

CHAPTER 5

CONCLUSION

An approach is proposed to perform blind source separation of spatially sparse frequency hopping RF sources with intermittent activity observed over a Spatial Channel Model in the following propagation environments: (*i*) LOS, (*ii*) single-cluster, (*iii*) multiple-cluster and (*iv*) LOS with interference.

In Chapter 1, the BSS problem of FH sources is introduced. The approaches to tackle similar problems available in current literature are discussed, along with the shortcomings of said approaches. ICA-based methods are not suitable for intermittent sources, and for cases where number of sources and sensors are not known. TFA-based methods suffer from spectral leakages, cross-term interference and high SNR requirements. These make them more useful as exploratory tools towards a more refined solution rather than a complete solution to estimate hop timings and frequencies blindly. ML-based techniques have lower SNR requirements, but are not scalable to multiple FH sources, making it a limited solution. These leads us to explore alternate approaches to our problem. It is also mentioned that the BSS problem with intermittent FH sources over LOS and NLOS channels has not been discussed before in literature, and that the purpose of this dissertation is to seek a way to bridge this gap.

In Chapter 2, the focus is on defining what is meant by spatially sparse and intermittent activity of the FH sources of interest. On-off patterns of each source change slowly but smoothly. The source activity is assumed to be governed by an HMM. The activity of each source is modeled after an independent HMM, where the hidden state at each time depends only on the hidden state preceding it. The parameters of the HMM are defined in detail as well. Observation models are

discussed for: (*i*) LOS model, (*ii*) single-cluster model, (*iii*) multiple-cluster model, and, (*iv*) LOS model with interference. Problem formulations are included in this chapter. Received signals in all propagation environments are defined mathematically, accounting for differences in their observation models.

In Chapter 3, the set of unknowns which we aim to find are listed. The goal of our work is to determine for each source, the activity pattern and the pattern of frequency hops. The received signal matrix is used to estimate FHs and DOAs (in the presence of angular spread, multipath components, and interference) over the course of the period of observation. A source's activity is estimated by using observations to extract DOA information versus time, and is used as a criteria for source separation. Our approach includes a FH estimation stage, a DOA estimation stage and a pairing stage that combines information from the previous stages to label the sources. The DOA and FH estimation stages exploit properties of intermittence of the source signals. Due to presence of multipath and clusters, different DOAs may be estimated corresponding to activity from one true source. Multiple activity patterns associated with different DOAs are considered "similar" if they match over a prescribed fraction of the time samples. The pairing stage uses the estimations from the previous stages to pick a pair of DOA and FH pattern that best fits the received signals at each time instant. The pairing assigns source labels to the signals and is capable of reducing false alarms that arise in the individual stages. The filtering process, termed HSF, is used to enhance the accuracy of the activity estimates, and by extension, the accuracy of source separation.

In Chapter 4, the efficacy of the proposed approach is demonstrated through numerical results, generated through simulations. The main performance criterion is the receiver operating characteristic (ROC) in which the probability of correct detection is plotted against the probability of false alarm. ROCs are plotted to compare the performance of the FH estimation stage, DOA estimation stage and the

pairing stage with and without HSF. Two different HSF techniques are discussed, namely, MPE and MAP techniques. Performance is also plotted with respect to the number of spatially sparse and intermittent FH sources, and with respect to varying jammer to signal ratios. It is observed that the HSF techniques are successful in reducing the amount of false alarms, thereby improving source separation. It is also seen that the MAP based HSF outperforms the MPE based HSF in every case.

APPENDIX A

VITERBI ALGORITHM

The Viterbi algorithm provides an efficient way of finding the most likely state sequence in the maximum *a posteriori* probability of a state sequence of a finite-state discrete-time Markov process. The Viterbi algorithm is a dynamic programming approach whose purpose is to make an inference based on a HMM model and observed data.

Consider a HMM with parameter $\Omega = (\mathbf{A}, \mathbf{B}, \pi)$ where $\mathbf{A}$ is the state transition probability matrix, $\mathbf{B}$ is the observation probability matrix, and π is the initial probability matrix. The hidden state sequence is denoted by $s(1:T)$ and the observed state sequence is denoted by $z(1:T)$. State transition probabilities are represented by the state transition matrix $\mathbf{A} = \{a_{ij}\}, j = 0, 1$ where the state transition probability distribution is given by $a_{ij} = P(s(t) = j | s(t-1) = i)$. Observation symbols probabilities are represented by the observation matrix $\mathbf{B} = \{b_j(k)\}, j, k = 0, 1$ where $b_j(k)$ denotes the observation symbol probability distribution in state j, $b_j(k) = P(z(t) = k | s(t) = j)$. We use the notation $b_j(z(t))$ to indicate the probability of observed value $z(t)$ conditioned on $s(t) = j$, $b_j(z(t)) = P(z(t) | s(t) = j)$. The initial state probability distribution is $\pi = \{\pi_0, \pi_1\}$, where $\pi_0 = P(s(1) = 0)$ and $\pi_1 = P(s(1) = 1)$.

Define the joint probability of the most likely path that ends at state i at time t, generating observations $z(1:t)$

$$\delta_i(t) \triangleq \max_{s(1:t-1)} P(s(1:t-1), s(t) = i | z(1:t), \Omega) \tag{A.1}$$

A recursive expression for this probability is obtained noting that if $\delta_i(t-1)$ is known, then $\delta_j(t)$ may be computed by accounting for the transition from state i at time $t-1$

to a state j at time t. This probability may be computed using quantities previously defined according to

$$\delta_j(t) = (\max_i \delta_i(t-1))a_{ij})b_j(z(t)) \tag{A.2}$$

The argument that maximizes Equation (A.2) is denoted by

$$\psi_j(t) \triangleq \arg\max_{i=0,1} (\rho_i(t-1)a_{ij}) \tag{A.3}$$

Following this procedure, the first state that can be determined as part of the most probable path is the final state $s(T)$, since any earlier determination may be affected by later times.

The recursive Viterbi algorithm is described below

1. Initialization:

$$\delta_i(1) = \pi_i b_i(z(1)),\ i = 0, 1 \tag{A.4}$$

$$\psi_i(1) = 0,\ i = 0, 1 \tag{A.5}$$

2. Recursion:

$$\delta_j(t) = (\max_i \delta_i(t-1)a_{ij})b_j(z(t)),\ 2 \leq t \leq T,\ j = 0, 1 \tag{A.6}$$

$$\psi_j(t) \triangleq \arg\max_{i=0,1} (\delta_i(t-1)a_{ij}),\ 2 \leq t \leq T,\ j = 0, 1 \tag{A.7}$$

3. Termination:

$$\hat{s}(T) = \arg\max_{i=0,1} (\delta_i(T)) \tag{A.8}$$

REFERENCES

[1] S. W. Golomb and G. Gong, *Signal Design for Good Correlation: For Wireless Communication, Cryptography, and Radar*, Cambridge, MA: Cambridge University Press, 2005.

[2] J. Jung and J. Lim, "Chaotic Standard Map Based Frequency Hopping OFDMA for Low Probability of Intercept," *IEEE Communications Letters*, vol. 15, no. 9, pp. 1019-1021, 2011.

[3] H. Wang, Yanlei Zhao, Feng Shen and Wei Sun, "The design of wide interval FH sequences based on RS code," *International Conference on Mechatronics and Automation*, Changchun, pp. 2345-2350, 2009.

[4] T. Chi and M. Chen, "A frequency hopping method for spatial RFID/ Wi-Fi/ Bluetooth scheduling in agricultural IoT," *Wireless Networks*, vol. 25, pp. 805–817, 2019.

[5] F. Olulana, "Coexistence of Wireless Avionics Intra-Communications Networks Based on Frequency Hopping with Collision Avoidance," *IEEE 38th International Conference on Electronics and Nanotechnology (ELNANO)*, Kiev, pp. 483-488, 2018.

[6] S. Yoo, J. Won, M. Seo and H. Cho, "Dynamic frequency hopping channel management in cognitive radio ad-hoc networks," *21st Asia-Pacific Conference on Communications (APCC)*, Kyoto, pp. 422-426, 2015.

[7] R. K. McLean, M. D. Silvius, K. M. Hopkinson, B. N. Flatley, E. S. Hennessey, C. C. Medve, J. J. Thompson, M. R. Tolson and C. V. Dalton, "An Architecture for Coexistence with Multiple Users in Frequency Hopping Cognitive Radio Networks," *IEEE Journal on Selected Areas in Communications*, vol. 32, no. 3, pp. 563-571, 2014.

[8] A. Kanaa and A. Z. Sha'ameri, "A robust parameter estimation of FHSS signals using time-frequency analysis in a non-cooperative environment," *Physical Communication*, vol. 26, pp. 9–20, 2018.

[9] C. Ying, Z. Fei and G. Shuxu. "Blind Compressed Sensing Parameter Estimation of Non-cooperative Frequency Hopping Signal", *Journal of Radars*, vol. 5, no. 5, pp. 531-537, 2016.

[10] P. Comon and C. Jutten, *Handbook of Blind Source Separation: Independent Component analysis and Applications*, Cambridge, MA: Academic Press, 2010.

[11] H. Suzuki, "A Statistical Model for Urban Radio Propogation", *IEEE Transactions on Communications*, vol. 25, no. 7, pp. 673-680, 1977.

[12] L. Vuokko, V-M. Kolmonen, J. Salo and P. Vainikainen, "Measurement of Large-Scale Cluster Power Characteristics for Geometric Channel Models", *IEEE Transactions on Antennas and Propagation*, vol. 55, no. 11, pp. 3361-3365, 2007.

[13] K.V.S. Hari, B. Ottersten, "Parameter estimation using a sensor array in a Ricean fading channel", *Sadhana 23*, pp. 5–15, 1998.

[14] F. Adachi, M. T. Feeney, J. D. Parsons, and A. G. Williamson. "Crosscorrelation between the envelopes of 900 MHz signals received at a mobile radio base station site", *IEEE Proceedings F- Communications, Radar and Signal Processing*, vol. 133, no. 6, pp. 506-512. IET, 1986.

[15] 3rd Generation Partnership Project (3GPP), "Spatial channel model for multiple input multiple output (MIMO) simulations (3GPP TR 25.996 version 6.1.0 Release 6)," ETSI, Tech. Rep, 2003.

[16] 3rd Generation Partnership Project (3GPP), "Spatial channel model for multiple input multiple output (MIMO) simulations (3GPP TR 25.996 version 11.0.0 Release 11)," ETSI, Tech. Rep, 2012.

[17] 3rd Generation Partnership Project (3GPP), "Spatial channel model for multiple input multiple output (MIMO) simulations (3GPP TR 25.996 version 13.1.0 Release 13)," ETSI, Tech. Rep, 2016.

[18] Y. d. J. Bultitude, and R. Terhi, "IST-4-027756 WINNER II D1. 1.2 V1. 2 WINNER II Channel Models." EBITG, TUI, UOULU, CU/CRC, NOKIA, Tech. Rep (2007).

[19] 3rd Generation Partnership Project (3GPP), "5G; Study on channel model for frequencies from 0.5 to 100 GHz (3GPP TR 38.901 version 14.3.0 Release 14)," ETSI, Tech. Rep, 2018.

[20] V. Vakilian, J. -F. Frigon and S. Roy, "Direction-of-arrival estimation in a clustered channel model," *10th IEEE International NEWCAS Conference*, Montreal, QC, Canada, pp. 313-316, 2012.

[21] A. Hyvarinen and E. Oja, "Independent component analysis: algorithms and applications", *Neural Networks*, vol. 13, pp. 411–430, 2000.

[22] S. M. Alavi and W. B. Kleijn, "Distributed linear blind source separation over wireless sensor networks with arbitrary connectivity patterns", *IEEE International Conference on Acoustics, Speech, and Signal Processing (ICASSP)*, pp. 3171–3175, 2016.

[23] S. S. Ivrigh, S. M.-S. Sadough, and A. A. Ghorashi, A blind source separation technique for spectrum sensing in cognitive radio networks based on kurtosis metric", *1st International eConference on Computer and Knowledge Engineering (ICCKE)*, pp. 333–337, 2011.

[24] Z. Uddin, A. Ahmad and M. Iqbal, "ICA based MIMO transceiver for time varying wireless channels utilizing smaller data blocks lengths", *Wireless Personal Communications*, vol. 94, no. 4, pp. 3147-3161, 2007.

[25] J. Cardoso and B. H. Laheld, "Equivariant adaptive source separation", *IEEE Transactions on Signal Processing*, vol. 44, no. 12, pp. 3017-3030, 1996.

[26] M. R. DeYoung and B. L. Evans, "Blind source separation with a time-varying mixing matrix", *Asilomar Conference on Signals, Systems and Computers (ACSSC)*, pp. 1-5, 2007.

[27] J. A. Chambers, M. G. Jafari and S. McLaughlin, "Variable step-size EASI algorithm for sequential blind source separation", *Electronics Letters*, vol. 40, no. 6, pp. 393-394,2004.

[28] A. Dong, O. Simeone, A. M. Haimovich and J. A. Dabin, "Blind Sparse Estimation of Intermittent Sources Over Unknown Fading Channels", *IEEE Transactions on Vehicular Technology*, vol. 68, no. 10, pp. 9861-9871, 2019.

[29] A. Ghosh, "Blind source separation using dictionary learning over time-varying channels", MS Thesis, Electrical and Computer Engineering, New Jersey Institute of Technology, USA, 2019. [Online] Available at: https://digitalcommons.njit.edu/theses/1655

[30] A. Dong, A. Ghosh, A. Haimovich and J. Dabin, "Sparse Recovery of Intermittent Frequency Hopping Signals Aided by DOA", *54th Annual Conference on Information Sciences and Systems (CISS)*, pp. 1-6, 2020.

[31] A. Ghosh, A. Dong, A. Haimovich, O. Simeone and J. Dabin, "Blind Source Separation of Intermittent Frequency Hopping Sources over LOS and NLOS channels", *IEEE Transactions on Wireless Communications*, Submitted, 2023.

[32] A. Ghosh, A. Haimovich, and J. Dabin, "Interference Mitigation in Blind Source Separation by Hidden State Filtering", *57th Annual Conference on Information Sciences and Systems (CISS)*,pp. 1-6, 2023.

[33] H. Luan and H. Jiang, "Blind Detection of Frequency Hopping Signal Using Time-Frequency Analysis," *6th International Conference on Wireless Communications Networking and Mobile Computing (WiCOM)*, Chengdu, pp. 1-4, 2010.

[34] F. Javed and A. Mahmood, "The use of time frequency analysis for spectrum sensing in cognitive radios," *4th International Conference on Signal Processing and Communication Systems*, Gold Coast, QLD, pp. 1-7, 2010.

[35] K. Gröchenig, *Foundations of Time-Frequency Analysis*, New York, NY: Springer, 2013.

[36] B. Boashash, *Time-Frequency Signal Analysis and Processing: A Comprehensive Reference*. Waltham, MA: Elsevier, 2016.

[37] Y. Yang, Z. Peng, W. Zhang, G. Meng, "Parameterised Time-Frequency Analysis Methods and their Engineering Applications: A Review of Recent Advances," *Mechanical Systems and Signal Processing*, vol. 119, pp. 182-221, 2019.

[38] K. Lee and S. Oh, "Detection of Frequency-Hopping Signals with Deep Learning," *IEEE Communications Letters*, vol. 24, no. 5, pp. 1042-1046, 2020.

[39] A. Valyrakis, E. E. Tsakonas, N. D. Sidiropoulos and A. Swami, "Stochastic Modeling and Particle Filtering Algorithms for Tracking a Frequency-Hopped Signal," *IEEE Transactions on Signal Processing*, vol. 57, no. 8, pp. 3108-3118, 2009.

[40] C. C. Ko, Wanjun Zhi and F. Chin, "ML-based frequency estimation and synchronization of frequency hopping signals," *IEEE Transactions on Signal Processing*, vol. 53, no. 2, pp. 403-410, 2005.

[41] X. Liu, N. D. Sidiropoulos, and A. Swami, "Joint hop timing and frequency estimation for collision resolution in FH networks," *IEEE Transactions on Wireless Communications*, vol. 4, pp. 3063–3074, 2005.

[42] D. Angelosante, G. B. Giannakis, and N. D. Sidiropoulos, "Estimating multiple frequency hopping signal parameters via sparse linear regression," *IEEE Transactions on Signal Processing*, vol. 58, pp. 5044–5056, 2010.

[43] X. Liu, N. D. Sidiropoulos and A. Swami, "Blind high-resolution localization and tracking of multiple frequency hopped signals," *IEEE Transactions on Signal Processing*, vol. 50, no. 4, pp. 889-901, 2002.

[44] Z.-C. Sha, Z.-M. Liu, Z.-T. Huang, and Y.-Y. Zhou, "Online Hop Timing Detection and Frequency Estimation of Multiple FH Signals," *ETRI Journal*, vol. 35, no. 5, pp. 748-756, 2013.

[45] W. Fu, Y. Hei and X. Li, "UBSS and blind parameters estimation algorithms for synchronous orthogonal FH signals," *Journal of Systems Engineering and Electronics*, vol. 25, no. 6, pp. 911-920, 2014.

[46] C. Zhang, Y. Wang and F. Jing, "Underdetermined Blind Source Separation of Synchronous Orthogonal Frequency-Hopping Signals Based on Tensor Decomposition Method," *IEEE Access*, vol. 6, pp. 69407-69414, 2018.

[47] S. Wei, M. Zhang, G. Wang, X. Sun, L. Zhang and D. Chen, "Robust Multi-Frame Joint Frequency Hopping Radar Waveform Parameters Estimation Under Low Signal-Noise-Ratio," *IEEE Access*, vol. 7, pp. 177198-177210, 2019.

[48] E.J. Im, K. Yelick, and R. Vuduc, "Sparsity: Optimization framework for sparse matrix kernels," *International Journal of High Performance Computing Applications*, vol. 18, no. 1, pp. 135–158, 2004.

[49] K. P. Murphy, *Machine Learning: A Probabilistic Perspective*, Cambridge, MA: MIT Press, 2012.

[50] L. R. Rabiner, "A tutorial on hidden Markov models and selected applications in speech recognition," *Proceedings of the IEEE*, vol. 77, no. 2, pp. 257-286, 1989.

[51] G. D. Forney, "The Viterbi algorithm", *Proceedings of the IEEE*, vol. 61, no. 3, pp. 268-278, 1973.

[52] S. Sahnoun, E.-H. Djermoune, C. Soussen, and D. Brie, "Sparse multidimensional modal analysis using a multigrid dictionary refinement," *EURASIP Journal on Advances in Signal Processing*, vol. 60, pp. 1–10, 2012.